

SUPPLEMENTARY APPENDIX

Table of Contents

A) Semi-automated gene discovery bioinformatics pipeline	4
B) Case reports	7
Novel and candidate genes for treatable neuro-metabolic diseases	7
Other novel & candidate genes	7
Expanding the phenotypic spectrum in rare genetic disorders	11
Unbiased WES approach allows discovery of unexpected results	12
C) Experimental data.....	14
D) Supplementary Discussion.....	26
E) Supplementary Acknowledgements.....	27
F) Supplementary Figures	28
Figure S1: Pedigrees and electropherograms of families with known pathogenic variants.....	28
G) Supplementary Tables	30
Table S1: Clinical Characteristics of the 50 Patients in 41 families.....	30
Table S2. Pathogenicity of variants according recent Standards and Guidelines of the American College of Medical Genetics Guidelines.....	31
Table S3: Known pathogenic variants.....	31
Table S4: Gene categories and corresponding patient phenotypes.....	32
Table S5: Blended phenotypes resulting from two single gene defects.....	42
H) Supplementary References	43

Supplementary Appendix To:

Exome Sequencing and the Management of Neuro-metabolic Disorders

Maja Tarailo-Graovac^{a,c}, Casper Shyr^{a,c}, Colin J. Ross^{b,c,e}, Gabriella A. Horvath^{c,d,e}, Ramona Salvarinova^{d,e}, Xin C. Ye^{a,c}, Lin-Hua Zhang^{a,e}, Amit P. Bhavsar^{c,e}, Jessica JY Lee^{a,c}, Britt I Drögemöller^{a,c,e}, Mena Abdelsayed^f, Majid Alfadhel^g, Linlea L. Armstrong^{b,c}, Matthias R. Baumgartner^h, Patricie Burda^h, Mary B. Connolly^{c,e,i}, Jessie Cameron^j, Michelle Demos^{c,e,i}, Tammie Dewan^e, Janis Dionne^{c,e,k}, A. Mark Evans^l, Jan. M. Friedman^{b,c}, Ian Garber^{a,c}, Suzanne Lewis^{b,c}, Jiqiang Ling^m, Rupasri Mandalⁿ, Andre Mattman^o, Margaret McKinnon^{b,c}, Aspasia Michoulas^{e,i}, Daniel Metzger^{c,e,p}, Oluseye A. Ogunbayo^l, Bojana Rakic^q, Jacob Rozmus^{c,e,r}, Peter Ruben^f, Bryan Sayson^{d,g}, Saikat Santra^s, Kirk R. Schultz^{c,e,r}, Kathryn Selby^{c,e,i}, Paul Shekel^l, Sandra Sirrs^o, Cristina Skrypnik^t, Andrea Superti-Furga^u, Stuart E. Turvey^{c,e,v}, Margot I. Van Allen^{b,c}, David Wishart^{n,w}, Jiang Wu^m, John Wu^{c,e,r}, Dimitrios Zafeiriou^x, Leo Kluijtmans^y, Ron A. Wevers^y, Patrice Eydoux^{c,q}, Anna M. Lehman^{b,c}, Hilary Vallance^{c,q}, Sylvia Stockler-Ipsiroglu^{c,d,e}, Graham Sinclair^{c,q}, Wyeth W. Wasserman^{a,c}, Clara D. van Karnebeek^{a,c,d,e,†}

^aCentre for Molecular Medicine and Therapeutics, Vancouver, Canada; ^bDepartment of Medical Genetics, University of British Columbia, Vancouver, Canada; ^cChild & Family Research Institute, University of British Columbia, Vancouver, Canada; ^dDivision of Biochemical Diseases, BC Children's Hospital, Vancouver, Canada; ^eDepartment of Pediatrics, University of British Columbia, Vancouver, Canada; ^fDepartment of Biomedical Physiology and Kinesiology, Simon Fraser University, Burnaby, Canada; ^gDivision of Genetics, Department of Pediatrics, King Saud Bin Abdulaziz University for Health Sciences, King Abdulaziz Medical City, Riyadh, Saudi Arabia; ^hDivision of Metabolism and Children's Research Center, University Children's Hospital Zurich, Zurich, Switzerland; ⁱDivision of Pediatric Neurology, BC Children's Hospital, Vancouver, Canada; ^jDepartment of Pathology and Laboratory Medicine, Hospital for Sick Children, University of Toronto, Toronto, Canada; ^kDivision of Pediatric Nephrology, BC Children's Hospital, Vancouver, Canada; ^lCentre for Integrative Physiology, University of Edinburgh, Edinburgh, UK; ^mDepartment of Microbiology and Molecular Genetics, University of Texas Health Science Center, Houston, USA; ⁿDepartment of Biological & Computing Sciences, University of Alberta, Edmonton, Canada; ^oDivision of Endocrinology, University of British Columbia, Vancouver, Canada; ^pDivision of Pediatric Endocrinology, BC Children's Hospital, Vancouver, Canada; ^qDepartment of Pathology and Laboratory Medicine, University of British Columbia, Vancouver, Canada; ^rDivision of Hematology, Oncology & Transplantation, Michael Cuccione Childhood Cancer Research Program, BC Children's Hospital, Vancouver, Canada; ^sBirmingham Children's Hospital, Birmingham, U.K.; ^tAlJawahra Centre for Molecular Medicine and Inherited Disorders, Arabian Gulf University, Bahrain; ^uDepartment of Pediatrics, University of Lausanne, Lausanne, Switzerland; ^vDivision of Immunology, BC Children's Hospital, Vancouver, Canada; ^wNational Institute for Nanotechnology, Edmonton, Alberta, Canada; ^xDepartment of Pediatrics, Aristotle University of Thessaloniki, Thessaloniki, Greece

^yDepartment of Laboratory Medicine, Radboud University Medical Centre, Nijmegen, Netherlands;

[†]Correspondence to: Dr. van Karnebeek, Division of Biochemical Diseases, Rm K3-201, Department of Pediatrics, B.C. Children's Hospital, Centre for Molecular Medicine & Therapeutic, University of British Columbia 4480 Oak Street, Vancouver B.C. V6H 3V4, Canada or at cvankarnebeek@cw.bc.ca.

A) SEMI-AUTOMATED GENE DISCOVERY BIOINFORMATICS PIPELINE

The automated portion of the pipeline¹ starts with alignment of the FASTQ reads using the Bowtie2² aligner to the human reference genome version hg19 (restricted to reads with quality score 30 or higher), removal of duplicate reads by Picard, local re-alignment by Genome Analysis Toolkit (GATK)³, followed by variant calling using SAMtools⁴ on BAM files and annotation using SNPeff⁵. Semi-manual review of data quality is performed to confirm samples were consistent with expectations, including checking for correct sex and familial relationships; samples are also inspected for any evidence of cross-contamination (Fig. 1). The next automated step utilizes custom perl and python scripts to exclude variants attributable to sequencing errors (by comparing the frequency of called variants against our own database of more than 350 exomes processed by the pipeline; variants seen more than 10 times are excluded) or variants that are reported as frequent in dbSNP (<http://www.ncbi.nlm.nih.gov/snp>)⁶ (MEF > 1%). Subsequently the prioritization/ranking of the variants is performed based on: (1) frequency in the NHLBI Exome Sequencing Project (ESP) Exome Variant Server [EVS; (<http://evs.gs.washington.edu/EVS>)], (2) frequency of variants arising at the genic level using the FLAGS¹ approach, (3) predicted effect of the variants on protein function where nonsense, frameshift, missense, microdeletions, microduplications and splice-site variants are prioritized, (4) phred-scaled Combined Annotation Dependent Depletion [CADD; (<http://cadd.gs.washington.edu>)]⁷ and (5) match to clinician-supplied phenotype-related MeSH terms.

As family history does not appear to be informative for most patients in our study, we adopted an unbiased approach and considered all possible Mendelian inheritance models. We used custom scripts to group the identified, filtered, annotated and ranked variants according to their predicted mode of inheritance to homozygous recessive, hemizygous, compound heterozygous and *denovo*. The low coverage WES data are flagged as part of our automated pipeline and manually curated. Variants of interest that are within low coverage regions are tested using Sanger re-sequencing. Furthermore, although the mitochondrial genome is not specifically captured in the WES approach, a recent publication by Griffin et al., 2014⁸ demonstrated that mitochondrial DNA sequences can be reliably obtained using three different WES capture kits (Agilent SureSelect targeted capture kit used in this study is one of them). In some cases, for whom we did not identify a convincing candidate variant in the nuclear genome and who did not have mtDNA

sequencing done by a certified laboratory, we inspected the mitochondrial genome from the WES data. However, we did not identify any significant mitochondrial genome variants in these patients. The bioinformatics pipeline itself is designed to be unbiased, meaning that it is not influenced by the clinical phenotype, predicted candidate genes, predicted inheritance, negative clinical tests etc. The pipeline is run for each patient similarly, searching for all “impactful” rare variants considering all possible inheritance models. However, the final step of our gene-discovery approach is manual (Fig. 1) and performed in close collaboration between bioinformaticians and clinicians. The hallmark of this collaboration is the family form completed by the referring clinician that contains essential data on the patient phenotype along with a disease / pathway hypothesis. The manual bioinformatics steps include: (1) inspection of variants in each of the predicted modes of inheritance for quality using a genome browser, such as IGV [Integrative Genomics Viewer; (<https://www.broadinstitute.org/igv/>)]^{9,10}, (2) further assessment of deleteriousness of the variants using multiple tools, such as PolyPhen-2 (<http://genetics.bwh.harvard.edu/pph2/>)¹¹, PROVEAN (<http://provean.jcvi.org/index.php>)¹², MutationTaster (<http://www.mutationtaster.org>)¹³ and SIFT [Sorting Intolerant From Tolerant; (<http://sift.jcvi.org/>)]¹⁴ (3) analysis of the clinical phenotypes and literature related to the candidate gene, (4) manual curation of the literature supporting the evidence for variant classification in ClinVar (<http://www.ncbi.nlm.nih.gov/clinvar>) and/or Human Gene Mutation Database [HGMD; (<http://www.hgmd.org>)] and (5) manual inspection of the variant frequency in different ethnic sub-groups available at the Exome Aggregation Consortium [ExAC; <http://exac.broadinstitute.org/>]). The final list of variants includes the colour-coded flagged candidate genes based on the assigned bioinformatician’s interpretation as highly relevant (red), relevant (yellow) and unknown based on currently available data (not flagged); the lists are sent to clinicians for evaluation, followed by a multi-disciplinary meeting for the final selection of variants to be confirmed by Sanger re-sequencing and experimental validation (Fig. 1). Validation of pathogenicity and causality of variants in novel genes (previously unreported in human disease) were pursued according to the guidelines by MacArthur et al 2014¹⁵: identification of other families with the similar phenotype due to distinct variants segregating with a similar pattern of inheritance in the same gene, functional studies including rescue experiments in patient cells, well-established cell-lines and/or model organisms¹⁶. Variant classification into gene classes (novel, candidate and known) was done according to the report by

de Ligt et al 2012¹⁷: ‘novel’ for genes not previously implicated in human disease with 2 or more individuals with striking phenotypic overlap in unrelated families with damaging variants in the same gene, ‘candidate’ in case of only 1 identified family.

B) CASE REPORTS

Of note, for the two novel and 9 candidate human disease genes identified in our study, we take a stringent approach to validate the causal relationship of identified variants with the observed phenotype: identification of other families with similar phenotypes due to (other) variants in the same gene (currently we identified additional families for *CA5A* and *NANS*, while for others we continue to search for additional families), (*in vitro*) functional studies to demonstrate deleterious impact of the variant on protein function and pursuit of model organism studies. For novel phenotypes, we pursue one or more of these approaches. Case reports (below) and the experimental / biochemical data (Supplemental Materials, section C) are presented in the order of Table S3; these data are unpublished unless otherwise indicated.

NOVEL AND CANDIDATE GENES FOR TREATABLE NEURO-METABOLIC DISEASES

ACACB: Currently, validation of acetyl-coA carboxylase-beta deficiency (*ACACB*) deficiency as potentially novel IEM is underway. Preliminary results of *in vitro* studies indicate decreased enzymatic activity at 37°C of the mutated (compound heterozygous variants) acetyl-coA carboxylase-beta when compared to wildtype, as well as decreased stability at 40°C, in a 7 year-old boy with compound heterozygous *ACACB* (MIM 601557) variants presenting with speech delay and, since age 19 months recurrent fever-induced and biotin-responsive episodes of lethargy, lactic acidosis (pH 7.04; HCO³⁻6mmol/L) with metabolites suggestive of multiple carboxylase deficiency (Table 1). To explain the causal relation with the multiple-carboxylase deficiency phenotype, we postulate that since malonyl-CoA, generated by *ACACB* in mitochondria¹⁸, is a key regulator for fatty acid oxidation and energy homeostasis, the deficient *ACACB* activity alters the physiological conditions in mitochondria which in turn affects the function of multiple carboxylases. Additional experiments are ongoing.

The case reports for the 3 other potentially treatable neurometabolic diseases (due to recessive *CA5A*¹⁹, *GOT2* and *NANS*²⁰ variants) are presented in the main manuscript.

OTHER NOVEL & CANDIDATE GENES

RBSN: Another example is Rabenosyn-5 deficiency due to homozygous missense variant in *RBSN* (MIM 609511) in a 7-year old girl with intractable seizures, severe IDD, microcephaly,

dysostosis, osteopenia, craniofacial dysmorphism, macrocytosis and megaloblastoid erythropoiesis²¹. Her biochemical findings included transient cobalamin deficiency, severe hypertriglyceridemia following initiation of a ketogenic diet, microalbuminuria and partial cathepsin D deficiency. Patient fibroblasts showed decreased transferrin accumulation, proliferation rate, cytoskeletal and lysosomal abnormalities, all of which are consistent with a functional defect of this highly conserved multi-domain protein implicated in receptor-mediated endocytosis. Secondary disruption of multiple cellular functions dependent on endocytosis, likely results in severe multi-organ disease.

FAAH2: Another example is deficiency of fatty acid amide hydrolase 2 (FAAH2) due to hemizygous missense variant in *FAAH2* (MIM 300654), in a male with autistic features with an onset before the age of 2 years who subsequently developed additional features including anxiety, pseudoseizures, ataxia, supranuclear gaze palsy, and isolated learning disabilities as an adult²². FAAH2 plays a role in endocannabinoid degradation, and *in vitro* mutant fibroblast studies showed decreased enzyme activity as well as alterations in endocannabinoid levels and lipid metabolism²². We propose this novel condition might well explain a subset of X-linked neuropsychiatric disease.

SENPI: Furthermore, homozygous missense variants in *SENPI* (MIM 612157), which encodes an important desumoylation protein, were identified in a 4.5-year old girl who was born to non-consanguineous Iranian parents at gestational age 36weeks), presenting with microcephaly, intestinal atresia, seizure disorder, severe IDD, feeding difficulties with failure to thrive. MRI brain showed lissencephaly. At age 3 years, she developed severe bone marrow dysplasia and was diagnosed with acute myeloblastic leukemia. Chemotherapy was adapted according to the molecular diagnosis, with full recovery until this day. Western Blot showed decreased SENP1 protein, and functional abnormalities of B-cell were confirmed; sumoylation analyses are ongoing²³.

SYTL2: Furthermore, compound heterozygous *SYTL2* (MIM 612880, encoding SLP2a; synaptogamin like peptide 2a) variants were identified in a 38-year old female with learning disabilities, born to Caucasian non-consanguineous parents, who presented during adolescence

with splenomegaly and thrombocytopenia, and bone marrow findings of sea-blue histiocytes as well as histiocytes on splenic and liver pathology. The SYTL2 protein has an unspecified role that involves interactions with RAB27a (MIM 603868) to transport lysosome derived cytotoxic secretory vesicles, or melanosomes to the cell surface for exocytosis²⁴⁻²⁶. Autosomal recessive deficiency of RAB27a results in Griscelli syndrome type 2 (GS2; MIM 607624)²⁷. GS2 is associated with an immunologic deficiency affecting cytotoxic T-cell and NK cell function, leading to susceptibility to the hemato phagocytic lymphohistiocytosis (HLH) syndrome. Functional tests of this patient's NK cells and T-cells confirmed the predicted functional deficiencies observed in GS2 (see Table 2); the patient's splenomegaly and thrombocytopenia are also characteristic of this condition. Given the favorable effects of HSCT in GS2 patients on the frequency of HLH syndrome relapses²⁸, this invasive therapy could be considered in our patient once the SYTL2 deficiency was established as candidate diagnosis.

RYR3: Compound heterozygous *RYR3* (MIM180903) variants were identified in two siblings with moderate IDD, epilepsy, psychiatric disease, short stature, along with severe asthma and (intermittent) pulmonary hypertension. Ryanodine receptors, such as RYR3, are intracellular calcium ion release channels responsible for the release of Ca(2+) from intracellular stores following transduction of many different extracellular stimuli. Animal studies showed that lack of Ryr3-mediated Ca(2+) signaling results in abnormalities of certain neurons in the central nervous system²⁹ and deletion of *RYR3* impairs synaptic plasticity and learning in mice³⁰. Furthermore it is highly expressed in smooth muscle tissues such as the lung³¹. Thus, deficiency of this protein could well explain the neuropsychiatric and pulmonary phenotype in these siblings; and similarly to reports of RYR2 (MIM 180902) dysfunction in the pathogenesis of epilepsy^{32,33} and recently identified *de novo* variants in epilepsy patients³⁴ altered RYR3 gating could cause their seizures. Functional studies (depicted in Figure 1 show that variant E4693 is hyper-responsive to the RyR-selective calcium mobilizing messenger cyclic adenosine diphosphate-ribose (cADPR). We hypothesize that E3119K, when combined with E4693K, could indirectly enhance channel function further, by altering the capacity (either positively or negatively) with binding partners that either positively or negatively influence the capacity for channel activation by cADPR and / or calcium³⁵; further studies are underway. Drugs acting on

RyR channel complexes such as dantrolene and cADPR antagonists should be further explored in terms of usefulness for symptom management in our patients.

MFNG: Compound heterozygous missense variants in *MFNG* (MIM 602577) were identified in a 8-year old boy was born to non-consanguineous parents, who presented at age 1 year with stunted growth / short stature, facial dysmorphisms, translucent skin with erythematous patches on his legs and arms, diarrhea / cyclic vomiting, verbal apraxia, and moderate IDD. Urine amino acids showed a pattern suggestive of Hartnup Disease (MIM 234500). Manic Fringe is one of three human Fringe proteins, that acts in the Golgi as a glycosyltransferase enzyme that modifies the ability of Notch to bind to the Notch receptor. The Notch signaling pathway is important for cell-cell communication, which involves gene regulation mechanisms that control multiple cell differentiation processes during embryonic and adult life; impairments in this pathway have been reported to result in neuronal, skeletal, exocrine, gastro-intestinal and epidermal abnormalities³⁶, all present in our patient. *In vitro* studies confirmed reduced MFNG secretion of both mutants along with increased amount of mutant MFNG in cells, which lead to an enhanced MFNG activity, and indeed an alteration of Notch and Hey1 activity. Further functional studies are ongoing to further establish causality and understand pathophysiology.

NPL: Compound heterozygous *NPL* (MIM 611412) variants were identified in 19-year old male, born to healthy non-consanguineous Filipino parents, who presented with progressive dilated cardiomyopathy, mild skeletal myopathy and sensorineural hearing loss. Biochemical investigations revealed free sialicaciduria (Figure 2a,b); known genetic causes of aciduria were ruled out. His sister reportedly has mild muscle weakness, but has declined physical / cardiac exam; she was found to have sialicaciduria and the same *NPL* variants as her brother. CLIA-certified labs quantified the sialic acid (Neu5Ac) elevations; see the legend of Figure 2 for more detail. N-acetylneuraminase pyruvate lyase is a strong candidate given its function, i.e. to control the cellular concentration of sialic acid by catalyzing the conversion of sialic acid into acylmannosamines and pyruvate³⁷. Sialic acid in fibroblasts is markedly increased, and *in vitro* enzymatic measurements in mutant fibroblasts as well as model organism studies are underway. Importantly, studying phenotypes of other families with recessive *NPL* variants should elucidate the clinical phenotype of *NPL* deficiency. Of note the known pathogenic homozygous variant

explains the hearing loss in the index case (Figure S1E); father has the same genotype but no objectified hearing loss, and this could be explained by variable penetrance³⁸.

EXPANDING THE PHENOTYPIC SPECTRUM IN RARE GENETIC DISORDERS

Recently, we reported a male infant with a hemizygous missense variant in *PIGA* (MIM 311770), a gene encoding for phosphatidylinositol glycan, class A protein, presenting with dysmorphism, developmental arrest, infantile spasms, a pattern of lesion distribution on brain MRI resembling that typical of Maple Urine Syrup Disease, elevated alkaline phosphatase, mixed hearing loss (a combination of conductive and sensorineural), liver dysfunction, mitochondrial complex I and V deficiency, and therapy-responsive dyslipidemia with confirmed lipoprotein lipase deficiency³⁹. Our case helped to further delineate the heterogeneous phenotype of germline *PIGA* variants for which we proposed the term ‘*PIGA* deficiency’³⁹ and to expanded the spectrum of this disorder³⁹.

Further illustrating phenotypic delineation, we recently reported on a boy with a 13bp hemizygous deletion in *PLP1* (MIM 300401), a gene encoding for proteolipid protein 1, or lipophilin, a primary constituent of myelin in the central nervous system. The boy presented with global developmental delay, spasticity, nystagmus, ataxia, and most notably severe hypomyelination of early myelinating structures (HEMS) which is in contrast with MRI characteristics of Pelizaeus-Merzbacher (MIM 312080) disease, also caused by *PLP1* alterations⁴⁰. Identification of the *PLP1* deletion in our patient and review of other patients with the distinct HEMS phenotype extend the phenotypic spectrum of *PLP1*-related disorders and led to discovery that these patients have variants that alter *PLP1/DM20* alternative splicing, impacting early myelination.

Finally, in this study we contributed to the characterization of a novel autosomal recessive syndrome due to bi-allelic variants in *SCN4A*, which encodes the α -subunit of the skeletal muscle voltage-gated sodium channel (Nav1.4)⁴¹. This channel is essential for the generation and propagation of action potentials which initiate skeletal muscle contraction. Dominant gain of function mutations in *SCN4A* are a well-established cause of myotonia and periodic paralysis. In 2 siblings born to non-consanguineous parents and another 9 individuals from 5 unrelated kindreds, all presenting with congenital myopathy with onset *in utero*, recessive *SCN4A* mutations were identified via WES. In a subset of patients, including the youngest sib in our

family, perinatal death occurred, while the remaining case (including our currently 8-year old index) suffered marked congenital hypotonia and weakness, early-onset respiratory and swallowing difficulties, spinal deformities, but clear clinical improvement over time. Functional validation for the compound heterozygous *SCN4A* variants in our family included reverse transcriptase (RT)-PCR confirming a premature stop codon rendered by the splice site variant (Figure 3a), significant alteration in the biophysical properties (conductance, current density) of the encoded $\text{Na}_v1.4$ caused by the missense variant (Figures 3b and c).

UNBIASED WES APPROACH ALLOWS DISCOVERY OF UNEXPECTED RESULTS

The above patient presenting with severe hypomyelination of early myelinating structures (HEMS) (Table S3) illustrates how *unbiased* WES allows for discovery of the unexpected. Given the strong clinical suspicion, targeted Sanger sequencing of *PLP1* gene in a CLIA-certified laboratory was performed but yielded negative results. Our WES analysis uncovered a 13bp deletion within the *PLP1* gene, which was later acknowledged by the laboratory that had missed the variant initially prompting a change in their protocol. Thus in some cases, sensitivity achieved by proper WES analysis exceeds that of targeted Sanger sequencing. Another example is a female teenage patient presenting with dysmorphisms, short stature, dysautonomia, paroxysmal episodes, syncope, migraines and mild ID in whom a *de novo* heterozygous nonsense variant was identified in the *KMT2A* (MIM 159555) gene, lysine-specific methyltransferase 2A that methylates histone H3 and is known to cause Wiedemann-Steiner syndrome (MIM 605130). The patient did not manifest the hairy elbows phenotype, a hallmark of the syndrome, and the syndrome was not considered by the referring clinician. However, after the discovery and confirmation of the *de novo* variant in the *KMT2A* gene, the parents explained that the patient had shaved hair from her elbows. This example illustrates unexpected events that can misdirect a candidate gene approach even in hands of skilled clinicians.

C) EXPERIMENTAL DATA

Novel Genes

CA5A (MIM 114761): see biochemical data in van Karnebeek et al., 2014¹⁹

NANS (MIM 605202): Urinary N-acetyl mannosamine, as measured by quantitative NMR spectroscopy in our case (at age 3 years) was highest (295 $\mu\text{mol}/\text{mmol}$ creatinine); in 5 unrelated other patients (all adults at the time of study) harbouring bi-allelic *NANS* variants, the urinary concentration of ManNAc ranged from 41 to 98 $\mu\text{mol}/\text{mmol}$ creatinine (reference < 10)²⁰.

Candidate Genes

ACACB (MIM 601557):

Table 1. Urine organic acid profile in the patient with compound heterozygous *ACACB* variants during metabolic decompensation suggestive of multiple carboxylase deficiency

Urine organic acids ($\mu\text{mol}/\text{mmol}$ creatinine)	Case	Reference range
3-OH-valeric acid	1,395	1-52
3-methylcrotonylglycine	36	<1
Tiglylglycine	34	<3
3-OH-propionic acid	30	2-28
Propionylglycine	6	<1
methylcitric acid	23	<13
lactic acid	4,723	7-94
2-me-3-OH-butyric acid	194	<30
glutaric acid	1040	<9
3-methyl-glutaconic acid	153	<13

RBSN (MIM 609511): see biochemical data in Stockler et al., 2014²¹

FAAH2 (MIM 300654): see biochemical data in Sirrs et al., 2015²²

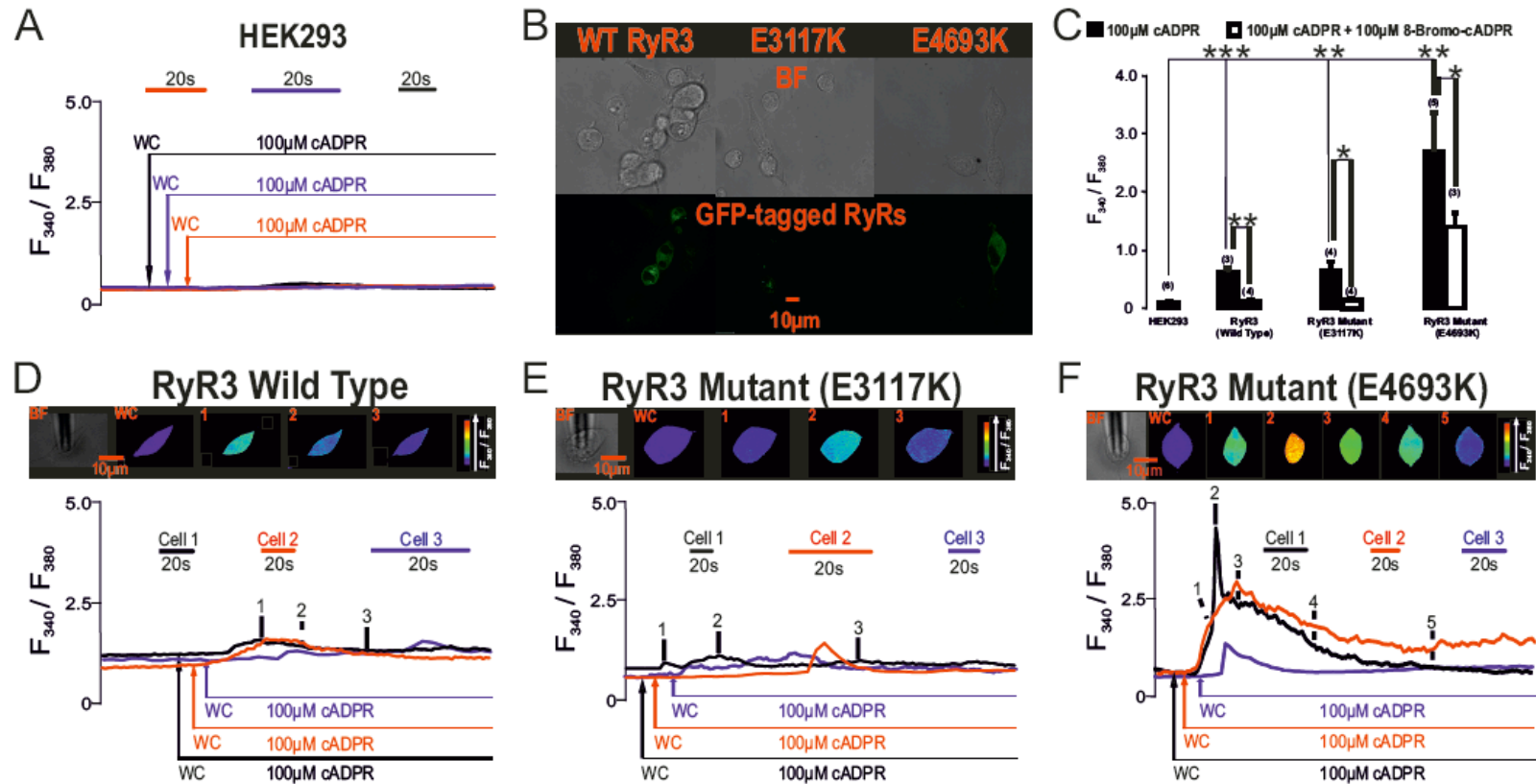
SYTL2 (MIM 612880)

Table 2. Functional data on the SYTL2 (SLP2a) loss of function variants. The CD107a mobilization fails to detect a normal amount of surface CD107a on stimulated lymphocytes indicating a defect in lymphocyte degranulation. The NK cell functional assays are abnormally low indicating impaired lytic capabilities of NK cells. The soluble CD163a protein level is abnormally high indicating macrophage activation.

Sample	Stimulated CD107a mobilization (flow cytometry) (%)	NK Cell Function Assay (Cr Release)%	NK Cell Function Assay (Cr release) Lytic Units	sCD163a (ng/ml)
index	6	9	1.2	2551
control	11-35	≥ 20	≥ 2.6	387-1785

RyR3 (MIM 180903)

Figure 1. RyR3 single point mutation E4693 is hyper-responsive to the RyR-selective calcium mobilizing messenger cyclic adenosine diphosphate-ribose.

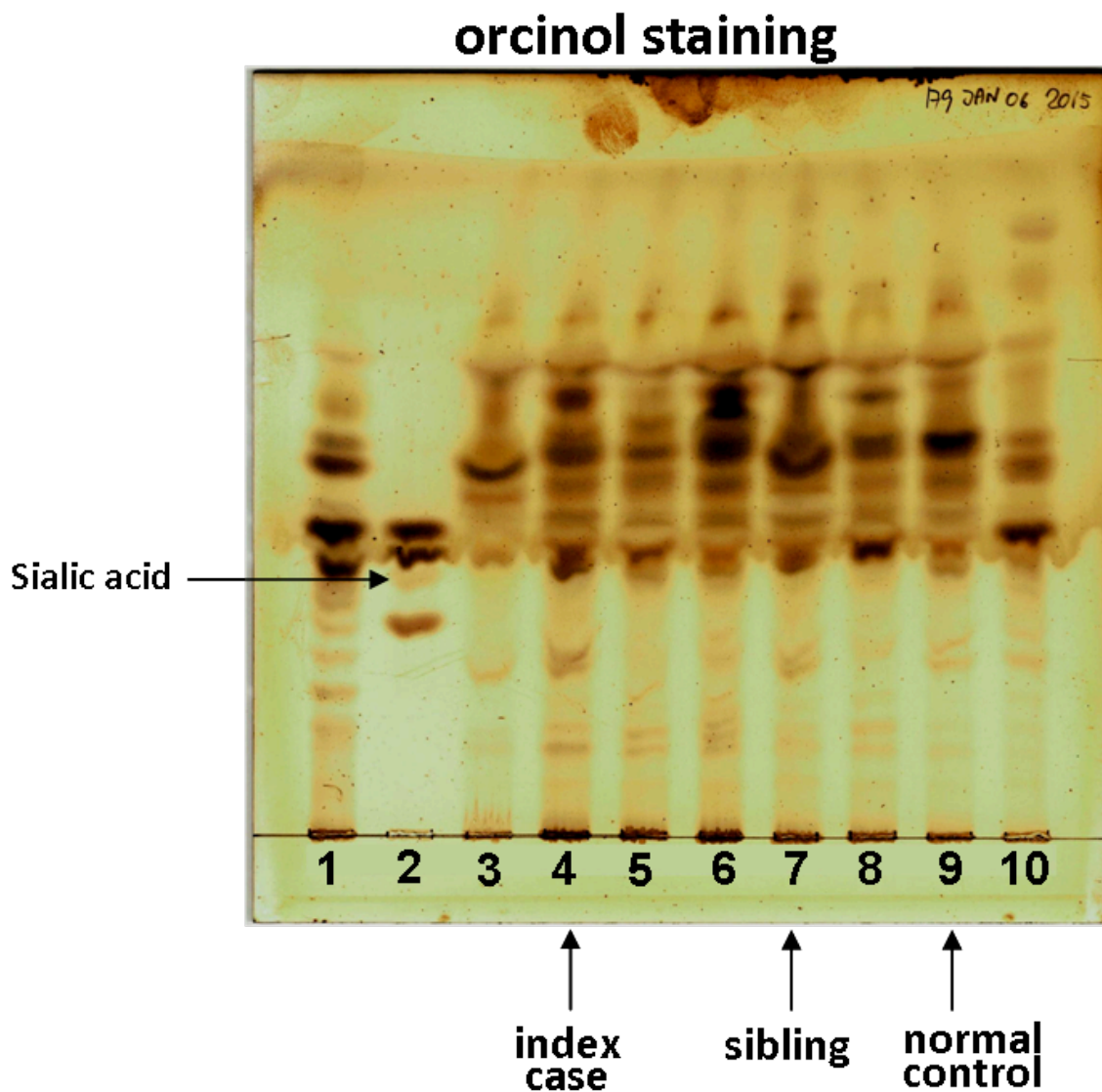


A) shows records of the F340/F380 ratio against time for 3 different HEK293 cells, which do not ordinarily express RyRs (1,2), during intracellular dialysis of 100 μ M cyclic adenosine diphosphate-ribose (cADPR); WC indicates the time point for onset of intracellular dialysis upon entering the whole-cell configuration using the patch-clamp technique. **B)** brightfield images (*upper panels*) and fluorescence images (*lower panels*) of HEK293 cells transiently transfected with GFP-tagged (**green**) wild type RyR3 (WT RyR3, *lefthand panel*), RyR3 mutant with single point mutation E3117 (*middle panel*) or RyR3 mutant with single point mutation E4693 (*righthand panel*). **C)** Bar chart shows the mean \pm SEM for the peak change in Fura-2 fluorescence ratio induced during intracellular dialysis of 100 μ M cADPR into wild type HEK293 cells and HEK293 cells expressing wild type RyR3 or mutant RyR3 incorporating single point mutations E4693 and E3117, respectively, in the absence and in the presence of 100 μ M 8-bromo-cADPR, a cADPR antagonist; data are means \pm SEM for at least 3 cells, with significance determined by two-sample *t* test between indicated groups (* <0.05 , ** <0.01 , *** <0.001). **D)** upper panel shows a bright field image (BF) of a HEK293 cell transiently transfected with wild type RyR3, and a series of pseudo-colour images of the Fura-2 fluorescence ratio (F340/F380) recorded in the same cell during intracellular dialysis of 100 μ M cADPR. The lower panel shows the corresponding record (black) of the F340/F380 ratio against time, together with two additional records (**red** and **blue**) obtained from different cells. E and F, as in D but for HEK293 cells transiently transfected with mutant RyR3 incorporating single point mutations (E) E3117 and (F) E4693^{42,43}.

NPL (MIM 611412)

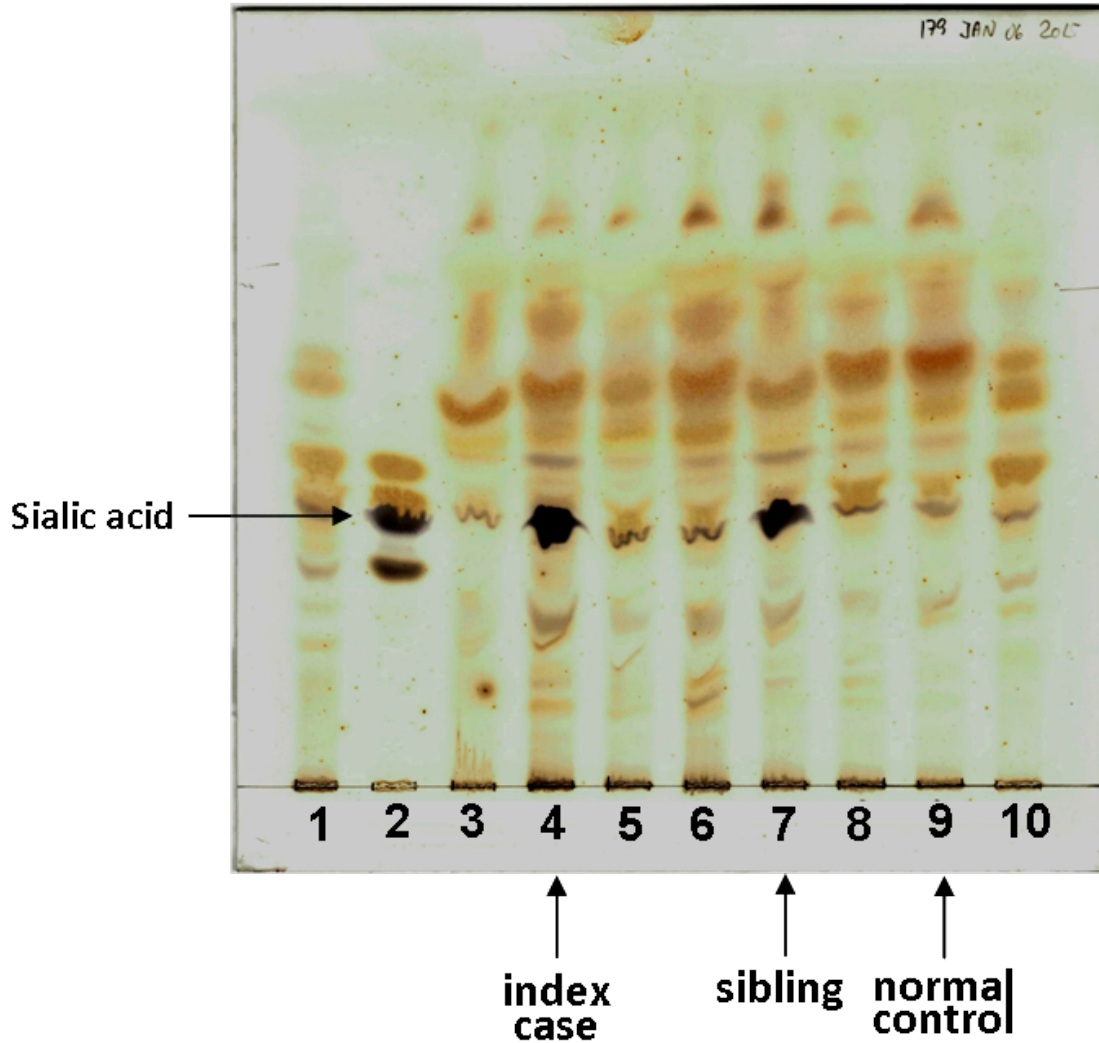
Figure 2. TLC urine oligosaccharides were abnormal for both index and affected sibling (a: TLC lanes 4 and 7 respectively) and revealed marked free sialicaciduria by resorcinol staining (b: lanes 4 and 7 respectively).

a)



b)

resorcinol staining



Further biochemical data: An abnormal concentration of Neu5Ac was determined by Q-TOF in urine and serum of the index case. Quantification of Neu5Ac in urine was performed by LC-MS/MS method on two different sample collections for the index: Neu5Ac= 122 $\mu\text{mol}/\text{mmol Cr}$ and Neu5Ac= 144 $\mu\text{mol}/\text{mmol Cr}$ (normal range for age>20 years: 9.7 \pm 8 $\mu\text{mol}/\text{mmolCr}$)⁴⁴ Urine Neu5Ac was quantified for q sample collection in the affected sibling by an HPLC method (1470 $\mu\text{mol}/\text{mg Cr}$; normal range 155-352 $\text{nmol}/\text{mg Cr}$) and by the LC-MS/MS method (Neu5Ac 139 $\mu\text{mol}/\text{mmol Cr}$; normal range for age>20 years: 9.7 \pm 8 $\mu\text{mol}/\text{mmolCr}$)⁴⁴.

Known genes with novel phenotypes

PIGA (MIM 311770): see biochemical data in Tarailo-Graovac et al., 2015³⁹

MTO1 (MIM 614667):

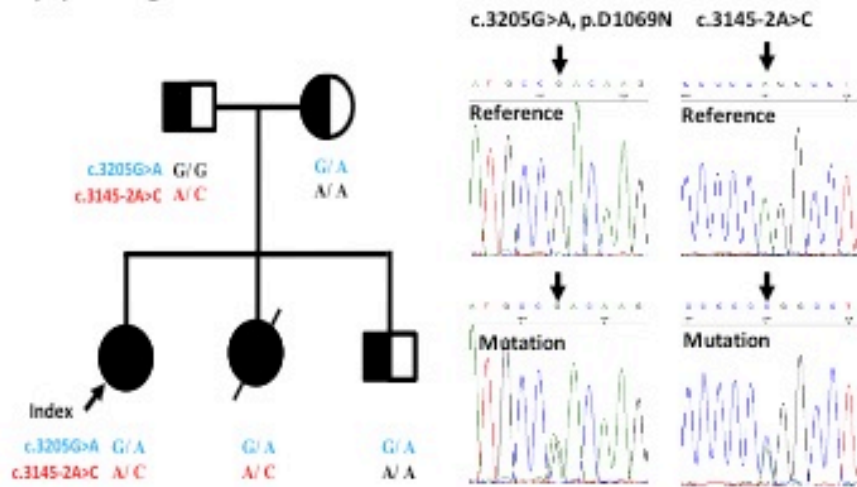
Table 3. Respiratory complex activities measured in muscle

	Affected sister	Reference interval	Index	Reference interval
Citrate Synthase (nmol/min/mg)	117	79-147	55 (L)	79-114
Complex I (nmol/min/mg)	11.3 (L)	16.6-61.6	4.1(L)	17.9-56.7
Complex I/Citrate Synthase	0.096 (L)	0.161-0.438	0.072(L)	0.134-0.469
Complex II (nmol/min/mg)	35.8	18.6-47.0	19.2(L)	22.4-44.8
Complex II/Citrate Synthase	0.305	0.194-0.388	0.349	0.168-0.387
Complex IV nmol/min/mg)	2.16 (L)	2.30-5.47	0.76(L)	2.30-5.03
Complex IV/Citrate Synthase	0.018 (L)	0.020-0.049	0.014(L)	0.017-0.036

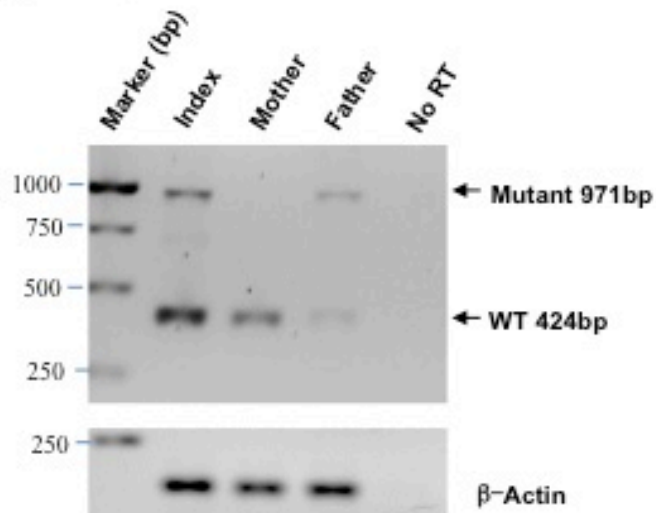
RMND1 (MIM 614917): see biochemical data in Janer et al., 2015⁴⁵

SCN4A(MIM 603967): Figure 3

(A) Pedigree



(B) RT-PCR



(C) Sequence analysis of RT-PCR products

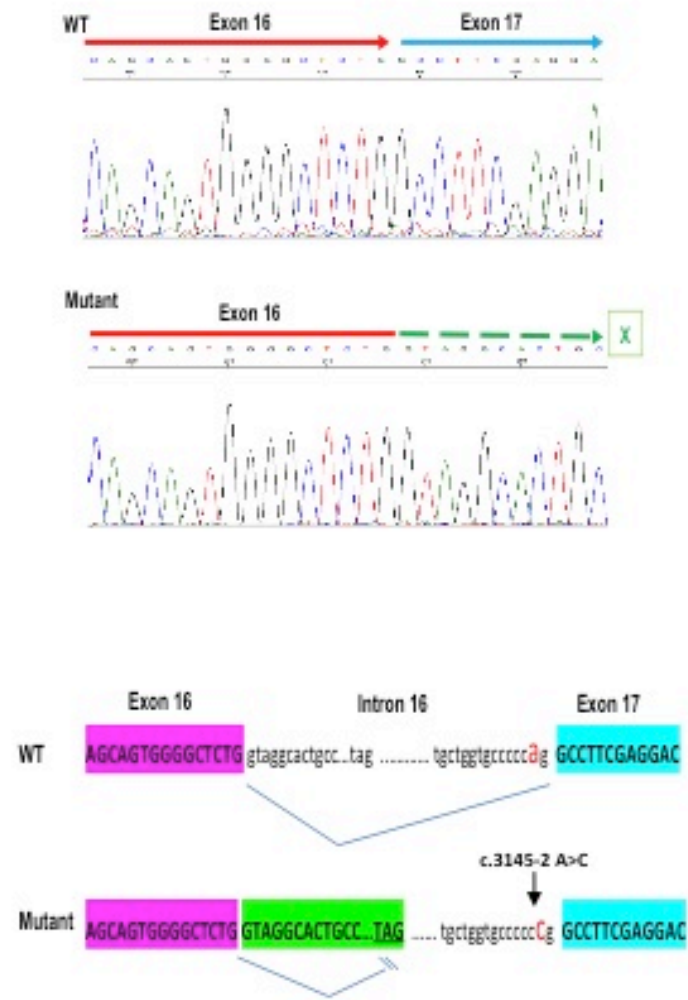
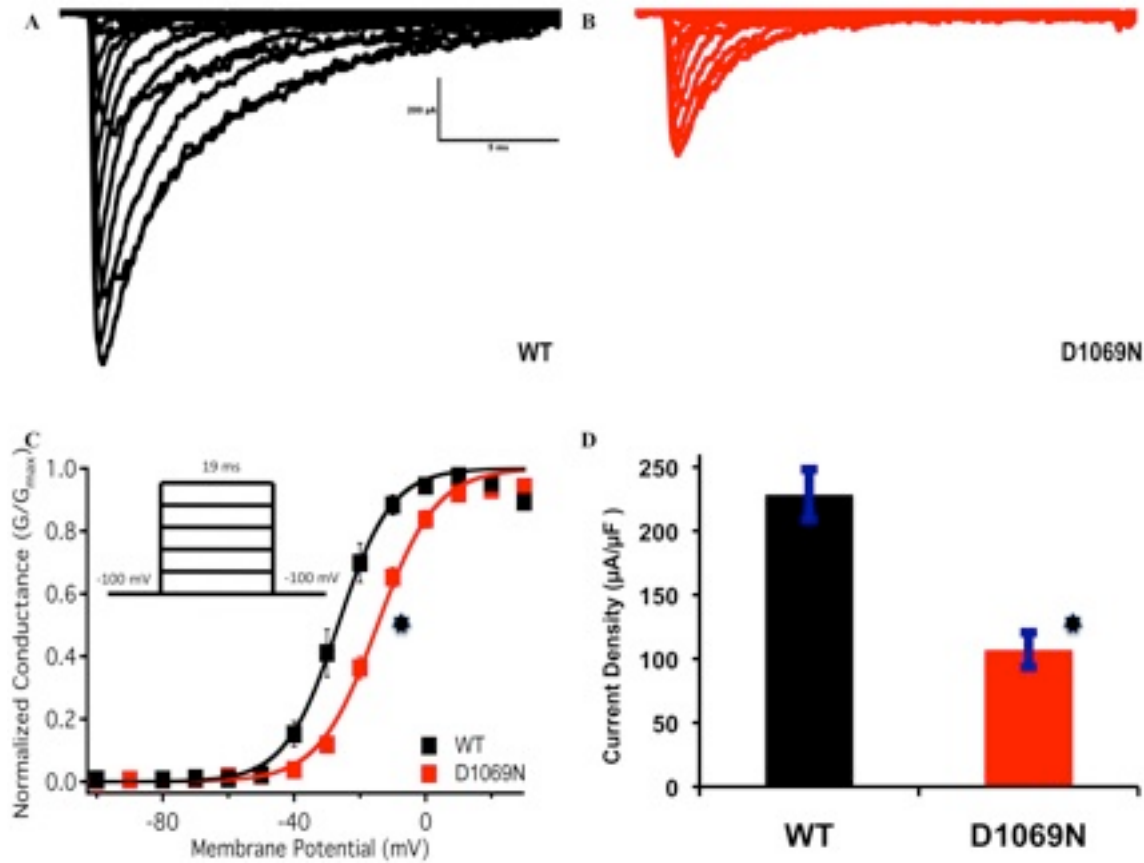


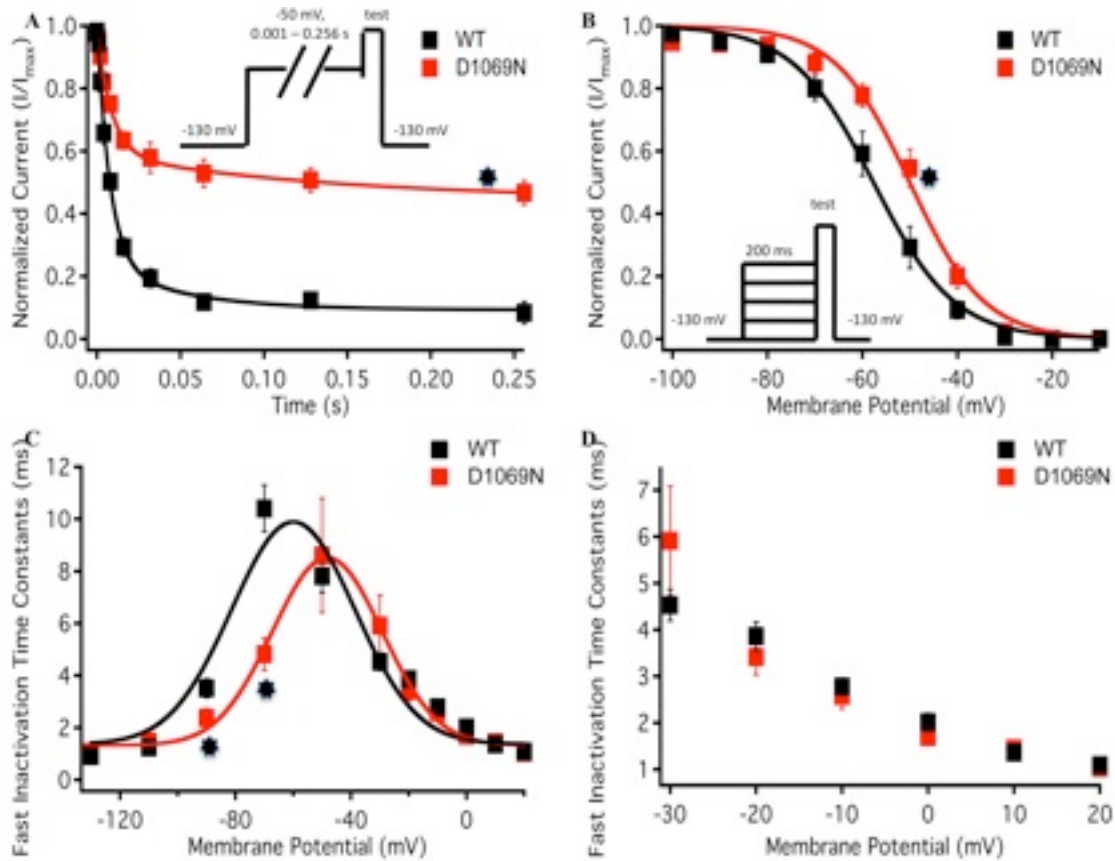
Figure 3a. The variant c.3145-2A>C in the *SCN4A* gene causes a splice site defect (p. Ala1049Val fs*50). **A.** Family pedigree showing two variants c.3205G>A, p.Asp1069Asn, (chr17: 62025363 C>T) and c.3145-2A>C (chr17: 62025425 T>G) investigated in this study. **B.** Reverse transcriptase (RT)-PCR analysis of *SCN4A* transcripts for variant c.3145-2A>C in RNA samples extracted from peripheral blood cells. Arrows indicate the products of different size amplified from RNA samples; No RT: as a negative control without the reverse transcriptase in RT reaction; beta-actin: a reference gene as a positive control for RT-PCR reaction. **C,** Sanger sequencing of RT-PCR products generated in (B). **Upper panel:** Sequence chromatograms, bars with arrow above the sequence chromatogram indicate exons 16/17 junction from 424bp band (WT); Bars with dotted lines indicate exon 16 at the junction with retained intron 16 from 971 bp band (Mutant). **Lower panel:** Depicted splicing events for wild type and mutation with intron 16 retention, leading to creation of a premature stop codon (underlined), along with the sequences denoted by each colour.

Figure S3b. Ex-vivo experiments showing current traces, normalized conductance and current density for SCN4A (Nav1.4) WT and p.Asp1069Asn; g.62025363 C>T) channel variants in transfected Chinese hamster ovary (CHO_{k1}) cells.



Panel A shows representative current traces of WT and Panel B for p.Asp1069Asn. Panel C shows normalized conductance plotted against membrane potential for both channel variants. The inset in Panel C shows the pulse protocol used to measure current amplitude at different voltages. Panel D shows the current density plotted in the form of a bar graph. * indicates statistical significance (Student's t-test, $p < 0.05$).

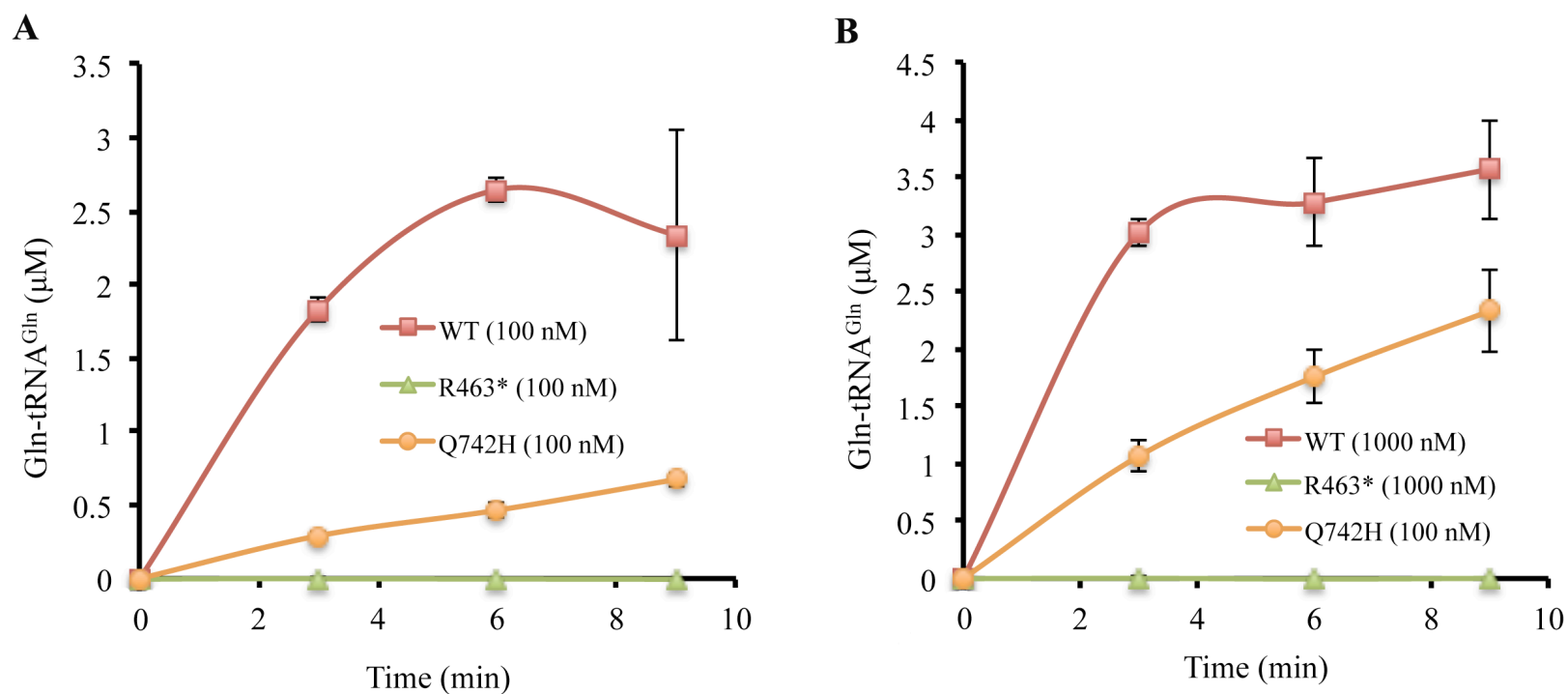
Figure 3c. Normalized current and fast inactivation time constants plotted against membrane potential for the SCN4A (Na_v1.4) WT and p.Asp1069Asn variants in transfected CHO_k1 cells.



Panel **A** shows the onset of fast inactivation performed at -50 mV as shown by the pulse protocol inset. Steady-state fast inactivation shown as normalized current plotted against membrane potential is shown in panel **B**. Panel **C** shows the fast inactivation time constants plotted against the membrane potential. These time constants are obtained from recovery, onset and IV protocols. Panel **D** shows a clearer view of the fast inactivation time constant curve shown in Panel **C** but within a limited voltage range (-30 mV to +20 mV). * indicates statistical significance ($p < 0.05$).

QARS (MIM 603727)

Figure 4. Aminoacylation activities of recombinant QARS variants.



Legend: Enzyme activity was undetectable in the p.Arg463*. Activity of p.Gln515His variants was decreased to lower than 10% of WT QARS. A. Aminoacylation activity was tested at the enzyme concentration of 100 nM. B. Aminoacylation activity was tested at the enzyme concentration of 1000 nM. Methods for production and purification of Recombinant Human QARS Proteins and QARS aminoacylation assays performed as described in previous study by Zhang, X et al. (2014)⁴⁶.

PCK1 (MIM 614168):

Table 4. PEPCK enzyme activity is shown for COS-1 cells transfected with empty vector, a vector containing either wildtype or mutant PCK1. Enzyme activity is shown \pm standard error, with the number of replicates in parentheses.

COS-1 Transfection experiment	PEPCK activity (nmol/mg/min)
COS-1	0.11 \pm 0.01 (3)
COS-1 + Empty vector	0.21 \pm 0.03 (4)
COS-1 + Wildtype <i>PCK1</i>	15.57 \pm 5.46 (4)
COS-1 + mutant <i>PCK1</i> (homozygous 12bp deletion)	0.23 \pm 0.04 (4)

D) SUPPLEMENTARY DISCUSSION

In 4 families, repeated semi-annual re-analysis of WES data failed to identify a genetic diagnosis; of note, mtDNA sequencing had been performed by a CLIA-certified laboratory in the probands of all 4 families without yielding variants of interest. Two of these 4 families were studied using proband-only WES, indicating a possibility that a pathogenic *de novo* variant was missed. Indeed, in one of these families by subsequently sequencing the parental exomes, we identified a novel *de novo* pathogenic variant in *MYLK* (MIM 600922), deemed causal of the phenotype. WGS analysis of the other family is underway. In 2 siblings presenting with a neurodegenerative phenotype and neurotransmitter abnormalities, whose seizures responded to Levocarbidoa and 5OH-tryptophan, duo-WES analysis failed to identify a diagnosis, ultimately attributed to inadequate coverage. Subsequent duo-WGS analysis revealed a previously described homozygous pathogenic variant (c.10G>C [p.Gly4Arg]) in *CSTB* (MIM 601145) resulting in Unverricht-Lundborg syndrome (MIM 254800). In the remaining family without a diagnosis, the proband presented with neonatal hyperammonemia, hyperlactatemia, methylmalonicaciduria which resolved completely, showing normal development and metabolic profiles at age 2 years; a large 600 gene panel and our trio-WES analysis did not yield disease-causing variants. Possibly this child does not suffer from a rare monogenic disease but a resolved immaturity of enzymes; we did not pursue further sequencing.

Preventive measures, such as metabolic diets, illustrate genomic diagnoses enable precision medicine. This is illustrated in our study by CA-VA deficiency¹⁹ and genetically confirmed cytosolic phosphoenolpyruvate carboxykinase deficiency.^{47, 48} which comes 40 years after first the clinical reports in 1975⁴⁹, in a 3-year old boy who presented with acute liver failure during gastro-intestinal illness, along with mild hypoglycemia, hyperammonemia with elevated glutamine, lactic acidosis, and elevated tricyclic acid metabolites. Here, we extend the hypoglycemia-lactic acidosis phenotype with acute liver failure during gastro-intestinal illness, and persistent signs of mitochondrial and urea cycle dysfunction amenable to treatment with a carbohydrate-rich diet and emergency regimen. *In vitro* mutant enzymatic activity in transfected COS-1 cells was markedly reduced (Table 4).

E) SUPPLEMENTARY ACKNOWLEDGEMENTS

We gratefully acknowledge the contributions of the following individuals: Dr. L. Bonafé and Dr. S. Unger, (University of Lausanne, Switzerland), Dr. U. Engelke and Dr. D. Lefeber (Radboud University Medical Centre, The Netherlands), Dr. M. Kaczocho, Dr. R. Haltiwänger and Ms. Shinako Kakuda (Stony Brook University, USA), Dr. G. Lavery (University of Birmingham, United Kingdom), Dr. A. Waheed and Dr. W. Sly (St. Louis University, USA), Dr. S. Corvera (University of Massachusetts Medical School, USA) for experimental studies; Mr. R. Houben (Health2Media) for graphics and digital applications; all team members of the Treatable Intellectual Disability Endeavour in British Columbia for contributions (www.tidebc.org), in particular Ms. S. Failanga, Ms. K. Withers, Ms. S. Schaumann, Ms. S. Lin, Ms. Sebastiano for nursing care and clinical coordination; Ms. B. Cheng, Ms. A. Giezen, Ms. K. Ueda for dietary management; Ms. B. Toh for metabolic sample handling; Ms. X. Han for Sanger sequencing; Dr. M. Thomas, Mr. T. Murphy, Ms. A. Ghani for consenting and data management; Ms. M. Higginson for DNA extraction and sample handling; Dr. A. Matthews for bio-informatics support; Mr. D. Arenillas and Mr. M. Hatas for systems support, and Ms. D. Pak, Ms. H. Cheung, Ms. E. Lomba, Ms. R. Giesbrecht (all affiliated with BC Children's Hospital and/or Centre for Molecular Medicine and Therapeutics, Child and Family Research Institute at the University of British Columbia) for research management support.

F) SUPPLEMENTARY FIGURES

Figure S1: Pedigrees and electropherograms of families with known pathogenic variants

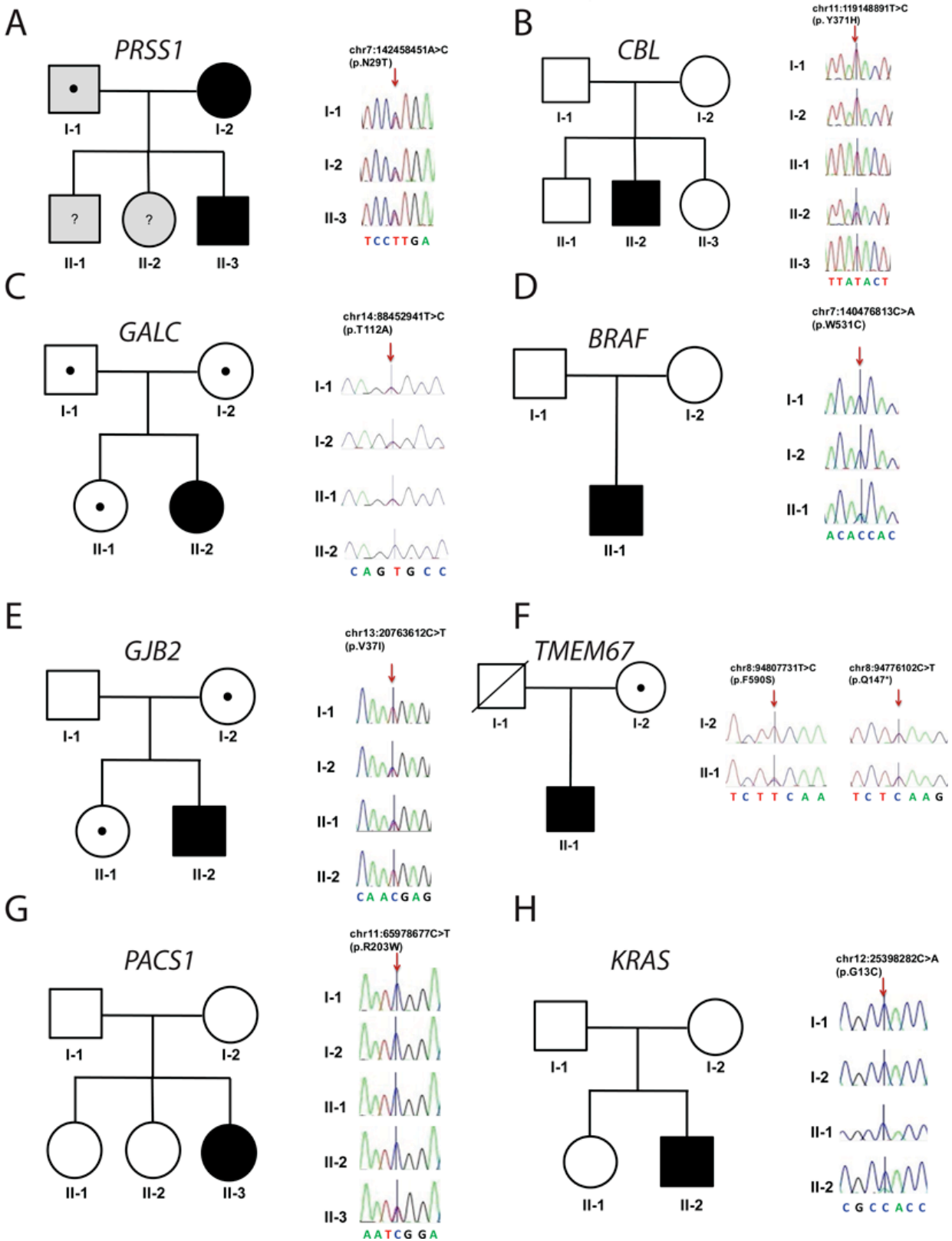


Figure Legend:

Unknown phenotypes are depicted in grey while unknown genotypes are depicted with question mark. The V37I variant in *GJB2* depicted in figure (E) has variable penetrance³⁸, providing an explanation for the father who is also homozygous for this variant but does not have an objectified hearing impairment.

G) SUPPLEMENTARY TABLES

Table S1: Clinical Characteristics of the 50 Patients in 41 families (41 probands, 9 siblings)	
Characteristics	Number of Patients (%)
Sex	
Male	29 (58%)
Female	21 (42%)
Age	
Child (< 19 yr)	44 (88%)
Adult (\geq 19 yr)	6 (12%)
Family structure (Patients from)	
Non-consanguineous families with a single affected child	30 (60%)
Non-consanguineous families with 2 affected children	14 (28%) (7 families)
Consanguineous families with a single affected child	2 (4%)
Consanguineous families with 2 affected children	4 (8%)
Number of siblings (affected siblings)	
0 (na)	10 (20%)
1 (5)	21 (42%)
2 (2)	13 (26%)
3 (2)	5 (10%)
4 (0)	1 (2%)
Population by descent	
European Caucasian	31 (62%)
East-Asian	3 (6%)
West-Asian	10 (20%)
South-Asian	4 (8%)
Latino	2 (4%)
Phenotype	
Intellectual developmental disorder (mild n=22; moderate n=17; severe-profound n=12)	50(100%)
Unexplained metabolic phenotype	49 (98%)
Abnormal neuro-imaging	30 (60%)
Abnormal Muscle Tone	23 (46%)
Seizure	15 (30%)
Abnormal Movement	13 (26%)
Epilepsy	12 (24%)
Psychiatric Symptoms	10 (20%)
Dysmorphic Features	8 (16%)
Cardiac Defect	8 (16%)
Short Stature	6 (12%)
Immune dysfunction	4 (8%)
Clinical genetic and biochemical analysis	
CMA (chromosomal microarray analysis)	36 (72%)
Targeted gene sequencing	34 (68%)
mtDNA sequencing	19 (38%)
Biochemical testing	50 (100%)

Table S2: Pathogenicity of variants according recent Standards and Guidelines of the American College of medical Genetics guidelines⁵⁰. The majority of the variants were classified as pathogenic (n=24[41%]) or likely pathogenic (n=17[29%]) according to recently published ACMG Standards and Guidelines.

[please be referred to: TableS2_ACMGClassificationsOfThe58Variants.xlsx]

Table S3: Known pathogenic variants

Gene	Disease [MIM]	Variant (hg19)
<i>PRSS1</i>	Pancreatitis, hereditary [MIM 16788]	g.142458451A>C (p.N29T) ⁵¹
<i>CBL</i>	Noonan syndrome-like disorder with or without juvenile myelomonocytic leukemia [MIM 613563]	g.119148891T>C (p.Y371H) ⁵²
<i>GALC</i>	Krabbe disease [MIM 245200]	g.88452941T>C (p.T112A) ⁵³
<i>GJB2</i>	Deafness, autosomal recessive 1A [MIM 220290]	g.20763612C>T (p.V37I) ^{38,54,55}
<i>TMEM67</i>	COACH syndrome [MIM 216360]	g.94807731T>C (p.F590S) ^{56,57}
<i>PACSI</i>	Mental retardation, autosomal dominant 17 [MIM 615009]	g.65978677 C>T (p.R203W) ⁵⁸
<i>KRAS</i>	Autoimmune lymphoproliferative syndrome type IV [MIM 614470]; Non-small cell lung cancer [MIM 211980]	g.25398282 C>A (p.G13C) ⁵⁹ g.25398282 C>A (p.G13C) ⁶⁰

Table S4: Gene categories and corresponding patient phenotypes

Gene	MIM	Phenotype + <i>metabolic specific</i>	Impact on clinical management	ACMG variant(s) classification (genotype)	Supporting Evidence	Literature (PMID)
A) Novel Genes						
<i>CA5A</i> §	615751	Neonatal hyperammonemia, hyperlactatemia, hypoglycemia; mild IDD; <i>hyperammonemia, hyperlactatemia, hypoglycemia, PCC and 3MCC deficiency metabolites</i>	Emergency dietary regimen & carnitine; avoid acetazolamide (resolution hyperammonemia & improved metabolic control)	Likely Pathogenic (Homozygous)	2 other families (same phenotype, different alleles); reduced enzyme activity (thermo-labile, unstable) in mutant transfected COS7-cells	24530203
<i>NANS</i> §§	*605202	Profound IDD, infantile spasms (hyposarrhythmia), developmental regression, coarse features, small basal ganglia with abnormal corpus callosum, hypomyelination, skeletal dysplasia; <i>lysosomal storage disease phenotype</i>	Potential - replacement CMP-sialic acid	Likely Pathogenic + Likely Pathogenic (Compound Heterozygous)	5 other families. Elevation precursors in urine, CSF, blood; reduced enzymatic activity in fibroblasts	10749855
B) Candidate Genes						
<i>ACACB</i> §§	*601557	Recurrent fever-induced metabolic crises (responsive to biotin), mild IDD; <i>suggestive of multiple carboxylase deficiency (lactic acidosis, elevated PCC and 3MCC metabolites)</i>	Biotin, anti-pyretics (improved metabolic control, avoidance crises)	Likely Pathogenic + Benign (Compound Heterozygous)	Single patient; reduced mutant enzyme activity (thermolabile) in patient cells	24740690
<i>RBSN</i> §	*609511	Severe IDD, coarse facial features, intractable seizures, microcephaly, dysostosis, osteopenia, macrocytosis and megaloblastoiderythropoiesis; <i>transient cobalamin deficiency, severe hypertriglyceridemia on ketogenic diet, partial cathepsin D deficiency</i>	None	Likely Pathogenic (Homozygous)	Single patient. Decreased transferrin accumulation, proliferation rate, cytoskeletal / lysosomal abnormalities in fibroblasts consistent with defect in receptor mediated endocytosis.	25233840

<i>GOT2</i>	*138150	Severe IDD, acquired microcephaly, severe epilepsy, spasticity, sleep disturbances, abdominal spasms; <i>low serum and CSF serine, lactic acidosis</i>	Oral pyridoxine & serine supplements (improved head growth, seizure control, psychomotor development)	Uncertain Significance + Uncertain Significance (Compound Heterozygous)	Single patient. Mechanistic fit & treatment response; stable isotope studies of malate-aspartate in patient cells & mouse model studies underway	16368075 22309504
<i>FAAH2§</i>	*300654	Learning disabilities, autism, anxiety, pseudo-seizures, ataxia, supranuclear gaze palsy; <i>abnormalities of serum acylcarnitine profile</i>	None	Likely Pathogenic (Hemizygous)	CNVs described in autism patients. Defect enzymatic activity in fibroblasts resulting in altered endocannabinoid profiles	20655035 25885783
<i>SENP1</i>	*612157	Severe IDD, congenital microcephaly, seizures, failure to thrive, intestinal atresia, acute myeloblastoid leukemia; <i>lissencephaly</i>	Chemotherapy (malignancy resolved)	Likely Pathogenic (Homozygous)	Single patient. Remaining candidate; decreased protein on Western Blot, abnormal functional B-cell studies.	2606032
<i>SYTL2§§</i>	*612880	Learning disabilities, Hemophagocytic lymphohistiocytosis, thrombocytopenia and splenomegaly (status post splenectomy), progressive liver dysfunction, skin hyperpigmentation; <i>lysosomal storage disease phenotype (blue histiocytes in spleen)</i>	Candidate for stem cell transplant	Uncertain significance + Uncertain significance (Compound Heterozygous)	Single patient. Confirmed immune deficiency affecting cytotoxic T-cell and NK-function defects as expected based on its interactions with RAB27a; model organism studies underway	15543135 17182843 18812475
<i>RYR3§§</i>	*180903	Moderate IDD, epilepsy, short stature, pulmonary hypertension, psychiatric disease; <i>sterol disorder</i>	None	Uncertain significance + Likely Pathogenic (Compound Heterozygous)	Two siblings with same phenotype. Mechanistic fit; functional studies in cell-lines underway	25126414
<i>MFNG</i>	*602577	Moderate IDD, epilepsy, apraxia, autism; dysmorphisms with asymmetric facies, stunted growth / short stature, cyclic vomiting, chronic diarrhea, erythematous skin lesions, <i>initial abnormal urine amino acids</i>	None	Likely Pathogenic + Likely Pathogenic (Compound Heterozygous)	Single patient Gain of function mutations; increase Notch and Hey1 activity	10935626

NPL§§	*611412	<i>Sibling 1</i> :cardiomyopathy, myopathy, <i>sialicaciduria</i> <i>Sibling 2</i> :not formally evaluated, mild myopathy , <i>sialicaciduria</i>	None	Likely Pathogenic + Likely Pathogenic (Compound Heterozygous)	Increased neuraminic acid in both siblings. Mechanistic fit; functional studies in fibroblasts underway.	16147865
-------	---------	--	------	---	---	----------

Legend to Tables S4A & B: *MIM corresponds to a gene as there is no disease associated with it at the time of the study; § biochemical / experimental data providing evidence for a deleterious effect of variants on protein function are either published in the listed PMID or presented as §§previously unpublished data in Supplemental Materials D.

C) Known Genes with Novel Phenotypes						
Gene	MIM	Known phenotype (PMID)	Patient Phenotype + <i>metabolic specific</i>	Novel features (PMID)#	Impact on clinical management (& clinical status)	ACMG variant(s) classification (genotype)
<i>CNKSR2</i>	*300724	IDD, limited or absent speech, seizures, hyperactivity, sleep disturbances (25223753)	Moderate IDD, language loss, epilepsy, sleep disturbances, dysautonomia, fatigue & cognitive decline responsive to choline therapy; <i>low acetyl choline levels</i>	Low acetylcholine levels responsive to therapy	Continuation pyridostigmine& choline (improved dysautonomia)	Uncertain significance (Hemizygous)
<i>SCN2A</i> §§	613721 607745	IDD, benign epilepsies, epileptic encephalopathy, hypotonia, hypersomnolence, movement disorder (23935176)	Severe IDD, autism, absent speech, acquired microcephaly, hypotonia, cortical & cerebellar atrophy, treatment-resistant seizures, <i>abnormal neurotransmitter monoamine profiles (low CSF HVA, 5-HIAA, pterins)</i>	Abnormal neurotransmitter monoamine metabolites (26647175)	Neurotransmitter supplements & refine AEDs (improved epilepsy control & communication)	Pathogenic (Heterozygous)
<i>PIGA</i> §	300868	IDD, epileptic encephalopathy, dysmorphisms, neuro-imaging abnormalities, +/- multi-organ involvement, elevated alkaline phosphatase (25885527)	†Profound IDD, Dysmorphisms, infantile spasms, contractures, brain intramyelin edema, mixed hearing loss,liver dysfunction; <i>lipoprotein lipase deficiency / mitochondrial complex I and IV deficiency / elevated alkaline phosphatase</i>	Lipoprotein lipase deficiency, Maple Syrup Disease-like features on brain MRI (25885527)	None	Likely Pathogenic (Hemizygous)
<i>CBL</i>	613563	Normal intellect or IDD, short stature, dysmorphisms, cardiac defect, predisposition to JMLL (20694012)	Mild IDD, ADHD, dysmorphic features, splenomegaly, thrombocytopenia; <i>storage disease phenotype</i>	Normal stature, splenomegaly, ADHD	Screening for malignancy (minimization morbidity)	Pathogenic (Heterozygous)
<i>ANO3</i>	615034	AD form of focal dystonia and myoclonus (DYT24) (24442708)	Moderate IDD, seizures, dystonia, hyperkinetic movements, microcephaly, sleep disturbances; <i>neurotransmitter profile abnormalities (low CSF HVA; low neopterin)</i>	abnormal neurotransmitter monoamine metabolites & recessive inheritance with IDD	Levo-carbidopamine& BH4 (improved movement disorder, sleep, seizure control)	Uncertain significance + Uncertain significance (Compound Heterozygous)

<i>DYRK1A</i>	614104	IDD, speech delay, seizures, microcephaly, growth delay & feeding problems (25920557)	Moderate IDD, intractable absence epilepsy, acquired microcephaly, failure to thrive; <i>GLUT-DS like phenotype (hypoglycorrhagia, low CSF:serum glucose ratio)</i>	GLUT1-DS phenotype responsive to ketogenic diet	None	Likely Pathogenic (Heterozygous)
<i>MTO1</i> §§	614702	Mitochondrial disease with IDD, myopathy, lactic acidosis, cardiac involvement (23929671)	2 sibs with moderate IDD, Treatment resistant epileptic encephalopathy, myopathy, recurrent rhabdomyolysis; seizure improvement on ketogenic diet <i>mitochondrial disease (respiratory chain complex I and IV deficiency)</i>	Rhabdomyolysis; adolescent onset cardiac involvement; seizures responsive to ketogenic diet	Ketogenic diet, mitochondrial cocktail; cardiac screening (improved seizure control & rhabdomyolysis)	Pathogenic + Pathogenic (Compound Heterozygous)
<i>RMND1</i> §	614922	Mitochondrial disease with IDD, lactic acidosis, encephalomyopathy (25604853)	† Severe IDD, congenital lactic acidosis, myopathy, hearing loss, renal failure, gastro-intestinal dysmotility, dysautonomia; <i>congenital lactic acidosis, severe combined mitochondrial respiratory chain deficiency</i>	Renal failure, deafness, dysautonomia (25604853)	None	Pathogenic + Pathogenic (Compound Heterozygous)
<i>AIMP1</i>	260600	Perlizaesus-Merzbacher-like disease with IDD, no acquisition of skills, microcephaly, seizures, hypomyelinating leukodystrophy, spasticity (24958424)	† Profound IDD, intractable epilepsy, developmental arrest, microcephaly, primary neurodegenerative disorder with secondary demyelination <i>leukodystrophy</i>	not Perlizaesus-Merzbacher-like (24958424)	None	Pathogenic (Homozygous)
<i>H6PD</i>	604931	Cortisone reductase deficiency with hypothalamic-pituitary-adrenal (HPA) axis activation and adrenal hyperandrogenism (23132696)	IDD secondary to myopathy, premature adrenarache, skin pigmentation abnormalities; <i>transient glycogen storage on muscle biopsy</i>	Skin pigmentation abnormalities	None	Uncertain significance + Uncertain significance (Compound Heterozygous)

<i>MED12</i>	309520 300895 305450	Opitz-Kaveggia syndrome Lujan-Fryns syndrome Ohdo syndrome, X-linked (24123922)	Moderate IDD, non-verbal, macrocephaly, dysmorphic features (prominent forehead, hypertelorism, broad thumbs), dysgenesis of corpus callosum, hypotonia, joint hypermobility <i>elevated leucine, isoleucine, valine (normalized during 2nd yr of life)</i>	Phenotypic features overlapping FG syndrome, Lujan-Fryns syndrome, and Ohdo syndrome	None	Likely Pathogenic (Hemizygous)
<i>SMAD4</i>	139210	IDD, dysmorphic facial features, microcephaly, square body shape, skeletal anomalies (broad ribs, iliac hypoplasia, brachydactyly, flattened vertebrae, thickened calvaria) Also congenital heart disease may occur. (26420300)	Severe IDD, short stature, microcephaly, square body shape, facial dysmorphisms, cyclic vomiting, congenital kidney abnormalities, <i>fluctuating hyperammonemia, hypoglycemia, ketosis (now resolved)</i>	Congenital kidney abnormalities, cyclic vomiting	Screening for small bowel & pancreatic cancer (minimization morbidity)	Pathogenic (Heterozygous)
<i>SCN4A</i> §§	170500 613345 614198 608390 168300	Dominant paramyotonia congenita, hyper- and hypo-kalemic periodic paralysis, and potassium aggravated myotonia (25839108)	2 sibs with IDD, congenital hypotonia, myopathy, respiratory & feeding insufficiency, abnormal EMG in both (older sib later in life improved albeit with Marfanoid dysmorphic features, kyphosis, joint hypermobility; †younger sib passed away); <i>mitochondrial respiratory complex I, II and IV deficiency</i>	Recessive congenital myopathy & fetal akinesia (26700687)	None	Pathogenic + Pathogenic (Compound Heterozygous)
<i>NDST1</i>	616116	IDD, delayed psychomotor development, delayed or absent expressive speech, seizures, hypotonia (25125150)	Moderate IDD, seizures, cranial nerve dysfunction, respiratory problems during infancy, facial dysmorphisms, hypotonia; <i>mitochondrial disease</i>	Cranial nerve dysfunction (<i>Am J Med Genet</i> 2016: in press)	None	Uncertain significance + Uncertain significance (Compound Heterozygous)

<i>PLPI</i>	312080 312920	Pelizaeus-Merzbacher disease, hypomyelinative leukodystrophy, IDDNystagmus, spastic quadriplegia, ataxia (25040584)	Severe IDD, progressive spasticity, nystagmus, ataxia, Perlizaeus-Merzbacher, severe hypomyelination of early myelinating structures (HEMS); <i>leukodystrophy</i>	'HEMS' (26125040)	None	Pathogenic (Hemizygous)
<i>QARS</i>	615760	IDD, hypo- / delayed myelination, thin corpus callosum, enlarged cerebral ventricles, small cerebellar vermis, intractable seizures, hypotonia, microcephaly, progressive neurodegeneration, (24656866)	Profound IDD with developmental arrest, progressive microcephaly with diffuse supra-tentorial cerebral atrophy & severely deficient myelination, intractable seizures; <i>serine deficiency</i>	Isolated supratentorial brain abnormalities (25432320)	None	Likely Pathogenic + Pathogenic (Compound Heterozygous)
<i>PCK1</i>	261680	Hypoglycemic episodes with lactic acidosis, secondary IDD and generalized seizures, liver steatosis, fatal liver failure; atrophy of the optic nerve (1092127)	Mild IDD, transient acute liver failure during viral illness, with episodes of recurrent hyperammonemia, lactic acidosis, elevated tricyclic acid metabolites, stabilization on responsive to carbohydrate rich diet, fatty liver infiltration; <i>recurrent metabolic decompensation</i>	transient acute liver failure disturbed urea cycle and mitochondrial function (<i>Molec Genet Metab</i> 2016: tentatively accepted)	Carbohydrate-rich diet (improved metabolic control & avoidance crises)	Likely Pathogenic (Homozygous)
<i>KCNQ2</i>	613720	IDD, epileptic encephalopathy, hypotonia and dystonia (26271793)	† Profound IDD, epileptic encephalopathy, hypotonia, dysautonomia, microcephaly; CSF GABA free 0.007 µmol/L (reference range: 0.017-0.067) CSF GABA total 4.300 µmol/L (reference range: 4.2-13.4) <i>low CSF GABA, mitochondrial complex I and II deficiency</i>	Low CSF GABA	None - patient deceased before GABA increasing agents could be started)	Pathogenic (Heterozygous)
<i>ATP2B3</i>	302500	IDD, hypotonia, cerebellar ataxia, dysarthria, slow eye movements, (22912398)	Mild IDD, autism, epilepsy, ataxia, improvement of neurologic symptoms on oral serine supplements; <i>low CSF and plasma serine</i>	Serine deficiency responsive to supplementation	Oral serine supplements (improved communication skills)	Uncertain significance (Hemizygous)

<i>EHMT1</i>	610253	IDD, absent speech, microcephaly, dysmorphic facial features, +/- congenital heart defects (22670141)	Severe IDD with regression, autism, hypotonia, dysmorphic facial features (incl. bilateral megalocornea); <i>neurodegeneration with loss of skills</i>	Megalocornea	None	Pathogenic (Heterozygous)
<i>TMEM67</i>	607361	IDD, abnormal eye movements, ataxia, cerebellar hypoplasia, hepatic fibrosis, coloboma, renal cysts (20232449)	Mild IDD, adolescent-onset dementia, vertical gaze palsy, ataxia, ADHD, cerebellar atrophy at age 8yrs (molar tooth sign at age 22yrs, after diagnosis established), hepatosplenomegaly, progressive hepatic fibrosis & portal hypertension,; <i>lysosomal storage disease phenotype</i>	Niemann-Pick C disease phenocopy with early-onset dementia	None	Pathogenic + Pathogenic (Compound Heterozygous)
<i>PACSI</i>	615009	IDD, characteristic facial dysmorphisms, seizures cardiac, cerebral, eye and kidney abnormalities (23159249)	Severe IDD, microcephaly, facial dysmorphisms, myopia, bifid uvula and submucous cleft, progressive ataxia and cerebellar atrophy, dysplastic pulmonary and aortic valves, failure to thrive; <i>neurodegeneration with progressive cerebellar atrophy</i>	Progressive cerebellar atrophy and ataxia (<i>AJMG 2016</i> : in press)	None	Pathogenic (Heterozygous)

Legend to Table S4C: *MIM corresponds to the gene; § biochemical / experimental data providing evidence for a deleterious effect of variants on protein function are either published in the listed PMID or presented as §§ previously unpublished data in Supplemental Materials D; † deceased; # novel phenotype of this cases published (PMID) or in press..

D) Known Genes with Known Phenotypes				
Gene	MIM	Phenotypic features + <i>metabolic specific</i>	Impact on clinical management & clinical status)	ACMG variant(s) classification
<i>MECP2</i>	312750	Severe IDD, epilepsy, autism, ataxia, developmental regression; <i>cerebral folate deficiency</i>	Folinic acid / stop betaine (improved seizure control)	Pathogenic (Heterozygous)
<i>MAT1A</i>	250850	Rett syndrome (<i>MECP2</i>); <i>high methionine</i>	n/a	Uncertain significance + Uncertain significance (Compound Heterozygous)
<i>KRAS</i> (somatic)	614470	Mild IDD, Rosai-Dorfman syndrome, chronic adrenal suppression, restrictive lung disease, chronic pain and depression, peribronchopulmonary dysplasia; <i>none</i>	Guided choice of mycophenolate mofetil	Pathogenic (Somatic)
<i>PRSS1</i>	167800	Pancreatitis, hereditary (& <i>RMND1</i> deficiency); <i>congenital lactic acidosis, severe combined mitochondrial respiratory chain deficiency</i>	Avoid triggers pancreatitis (cessation pancreatitis episodes)	Pathogenic (Heterozygous)
<i>KMT2A</i>	605130	Mild IDD, Dysmorphisms, short stature, hairy elbows, dysautonomia, paroxysmal episodes, syncope, migraines, fusion of C2-C3 vertebrae, 11 pairs of ribs, 5 th finger clinodactyly and camptodactyly; <i>low copper & ceruloplasmin</i>	None	Pathogenic (Heterozygous)
<i>GJB2</i>	220290	Moderate stable sensorineural hearing loss; <i>sialic aciduria</i>	None	Pathogenic (Homozygous)
<i>OSMR</i>	105250	Mild IDD, Severe early onset eczema (recessive), facial dysmorphism, and short stature (his growth is on the 15 th); <i>lysosomal storage phenotype</i>	None	Uncertain significance (Homozygous)
<i>PUF60</i>	615583	Mild IDD, Severe, early onset eczema (recessive), facial dysmorphism, and short stature (his growth is on the 15 th); <i>lysosomal storage phenotype</i>	None	Pathogenic (Heterozygous)

<i>GALC</i>	245200	IDD, Congenital hypotonia, myopathy, respiratory & feeding insufficiency, skin pigmentation abnormalities; <i>glycogen storage on muscle biopsy</i>	Consider hematopoietic stem cell transplant (none yet)	Pathogenic (Homozygous)
-------------	--------	---	--	----------------------------

Table S5: Blended phenotypes resulting from two single gene defects

Genes	Disease [MIM]	Phenotype (Omics2TreatID patient phenotype) + <i>metabolic specific</i>
<i>RMND1</i>	614922	Congenital lactic acidosis, severe myopathy, hearing loss, renal failure, and dysautonomia; <i>congenital lactic acidosis, severe combined mitochondrial respiratory chain deficiency</i>
<i>PRSSI</i>	167800	Pancreatitis, hereditary
<i>H6PD</i>	604931	Skin pigmentation abnormalities; <i>glycogen storage on muscle biopsy</i>
<i>GALC</i>	245200	Congenital hypotonia, respiratory & feeding insufficiency
<i>NPL</i>	Novel	<i>Cardiomyopathy, sialicaciduria</i> ; may be benign
<i>GJB2</i>	220290	Moderate stable sensorineural hearing loss
<i>MeCP2</i>	312750	ID, epilepsy, autism, ataxia, developmental regression, <i>Cerebral Folate deficiency</i> (Rett Syndrome)
<i>MATIA</i>	250850	<i>High methionine</i>
<i>OSMR</i>	105250	Severe, early onset eczema (Amyloidosis, primary localized cutaneous, recessive)
<i>PUF60</i>	615583	Facial dysmorphism, and short stature (Verheij syndrome)

H) SUPPLEMENTARY REFERENCES

1. Shyr C, Tarailo-Graovac M, Gottlieb M, Lee J, van Karnebeek C, Wasserman WW. FLAGS, frequently mutated genes in public exomes. *BMC Med Genomics* 2014;7(1):64.
2. Langmead B, Salzberg SL. Fast gapped-read alignment with Bowtie 2. *Nat Methods* 2012;9(4):357–9.
3. McKenna A, Hanna M, Banks E, et al. The Genome Analysis Toolkit: a MapReduce framework for analyzing next-generation DNA sequencing data. *Genome Res* 2010;20(9):1297–303.
4. Li H, Handsaker B, Wysoker A, et al. The Sequence Alignment/Map format and SAMtools. *Bioinforma Oxf Engl* 2009;25(16):2078–9.
5. Cingolani P, Platts A, Wang LL, et al. A program for annotating and predicting the effects of single nucleotide polymorphisms, SnpEff: SNPs in the genome of *Drosophila melanogaster* strain w1118; iso-2; iso-3. *Fly (Austin)* 2012;6(2):80–92.
6. Sherry ST, Ward MH, Kholodov M, et al. dbSNP: the NCBI database of genetic variation. *Nucleic Acids Res* 2001;29(1):308–11.
7. Kircher M, Witten DM, Jain P, O’Roak BJ, Cooper GM, Shendure J. A general framework for estimating the relative pathogenicity of human genetic variants. *Nat Genet* 2014;46(3):310–5.
8. Griffin HR, Pyle A, Blakely EL, et al. Accurate mitochondrial DNA sequencing using off-target reads provides a single test to identify pathogenic point mutations. *Genet Med Off J Am Coll Med Genet* 2014;16(12):962–71.
9. Robinson JT, Thorvaldsdóttir H, Winckler W, et al. Integrative genomics viewer. *Nat Biotechnol* 2011;29(1):24–6.
10. Thorvaldsdóttir H, Robinson JT, Mesirov JP. Integrative Genomics Viewer (IGV): high-performance genomics data visualization and exploration. *Brief Bioinform* 2013;14(2):178–92.
11. Adzhubei I, Jordan DM, Sunyaev SR. Predicting functional effect of human missense mutations using PolyPhen-2. *Curr Protoc Hum Genet Editor Board Jonathan Haines AI* 2013;Chapter 7:Unit7.20.
12. Choi Y, Chan AP. PROVEAN web server: a tool to predict the functional effect of amino acid substitutions and indels. *Bioinforma Oxf Engl* 2015;31(16):2745–7.
13. Schwarz JM, Cooper DN, Schuelke M, Seelow D. MutationTaster2: mutation prediction for the deep-sequencing age. *Nat Methods* 2014;11(4):361–2.
14. Kumar P, Henikoff S, Ng PC. Predicting the effects of coding non-synonymous variants on protein function using the SIFT algorithm. *Nat Protoc* 2009;4(7):1073–81.
15. MacArthur DG, Balasubramanian S, Frankish A, et al. A systematic survey of loss-of-function variants in human protein-coding genes. *Science* 2012;335(6070):823–8.

16. Hieter P, Boycott KM. Understanding rare disease pathogenesis: a grand challenge for model organisms. *Genetics* 2014;198(2):443–5.
17. de Ligt J, Willemsen MH, van Bon BWM, et al. Diagnostic exome sequencing in persons with severe intellectual disability. *N Engl J Med* 2012;367(20):1921–9.
18. Hwang I-W, Makishima Y, Kato T, Park S, Terzic A, Park EY. Human acetyl-CoA carboxylase 2 expressed in silkworm *Bombyx mori* exhibits posttranslational biotinylation and phosphorylation. *Appl Microbiol Biotechnol* 2014;98(19):8201–9.
19. van Karnebeek CD, Sly WS, Ross CJ, et al. Mitochondrial carbonic anhydrase VA deficiency resulting from CA5A alterations presents with hyperammonemia in early childhood. *Am J Hum Genet* 2014;94(3):453–61.
20. van Karnebeek C, Bonafé L, Wen X, et al. NANS-mediated synthesis of sialic acid is required for brain and skeletal development. *Nat Genet* 2016; doi 10.1038/ng.3578
21. Stockler S, Corvera S, Lambright D, et al. Single point mutation in Rabenosyn-5 in a female with intractable seizures and evidence of defective endocytotic trafficking. *Orphanet J Rare Dis* 2014;9(1):141.
22. Sirrs S, van Karnebeek CD, Peng X, et al. Defects in fatty acid amide hydrolase 2 in a male with neurologic and psychiatric symptoms. *Orphanet J Rare Dis* 2015;10(1):38.
23. Yamaguchi T, Sharma P, Athanasiou M, Kumar A, Yamada S, Kuehn MR. Mutation of SENP1/SuPr-2 reveals an essential role for desumoylation in mouse development. *Mol Cell Biol* 2005;25(12):5171–82.
24. Kuroda TS, Fukuda M, Ariga H, Mikoshiba K. The Slp homology domain of synaptotagmin-like proteins 1-4 and Slac2 functions as a novel Rab27A binding domain. *J Biol Chem* 2002;277(11):9212–8.
25. Kuroda TS, Fukuda M. Rab27A-binding protein Slp2-a is required for peripheral melanosome distribution and elongated cell shape in melanocytes. *Nat Cell Biol* 2004;6(12):1195–203.
26. Ménasché G, Ménager MM, Lefebvre JM, et al. A newly identified isoform of Slp2a associates with Rab27a in cytotoxic T cells and participates to cytotoxic granule secretion. *Blood* 2008;112(13):5052–62.
27. Ménasché G, Pastural E, Feldmann J, et al. Mutations in RAB27A cause Griscelli syndrome associated with haemophagocytic syndrome. *Nat Genet* 2000;25(2):173–6.
28. Rossi A, Borroni RG, Carrozzo AM, et al. Griscelli syndrome type 2: long-term follow-up after unrelated donor bone marrow transplantation. *Dermatol Basel Switz* 2009;218(4):376–9.
29. Takeshima H, Ikemoto T, Nishi M, et al. Generation and characterization of mutant mice lacking ryanodine receptor type 3. *J Biol Chem* 1996;271(33):19649–52.

30. Balschun D. Deletion of the ryanodine receptor type 3 (RyR3) impairs forms of synaptic plasticity and spatial learning. *EMBO J* 1999;18(19):5264–73.
31. Mattei MG, Giannini G, Moscatelli F, Sorrentino V. Chromosomal localization of murine ryanodine receptor genes RYR1, RYR2, and RYR3 by in situ hybridization. *Genomics* 1994;22(1):202–4.
32. Lehnart SE, Mongillo M, Bellinger A, et al. Leaky Ca²⁺ release channel/ryanodine receptor 2 causes seizures and sudden cardiac death in mice. *J Clin Invest* 2008;118(6):2230–45.
33. Nagrani T, Siyamwala M, Vahid G, Bekheit S. Ryanodine Calcium Channel: A Novel Channelopathy for Seizures. *The Neurologist* 2011;17(2):91–4.
34. De Novo Mutations in Synaptic Transmission Genes Including DNM1 Cause Epileptic Encephalopathies. *Am J Hum Genet* 2014;95(4):360–70.
35. Mackrill JJ. Ryanodine receptor calcium channels and their partners as drug targets. *Biochem Pharmacol* 2010;79(11):1535–43.
36. Yamamoto S, Schulze KL, Bellen HJ. Introduction to Notch signaling. *Methods Mol Biol Clifton NJ* 2014;1187:1–14.
37. Wu M, Gu S, Xu J, et al. A novel splice variant of human gene NPL, mainly expressed in human liver, kidney and peripheral blood leukocyte. *DNA Seq J DNA Seq Mapp* 2005;16(2):137–42.
38. Pollak A, Skórka A, Mueller-Malesińska M, et al. M34T and V37I mutations in GJB2 associated hearing impairment: evidence for pathogenicity and reduced penetrance. *Am J Med Genet A* 2007;143A(21):2534–43.
39. Tarailo-Graovac M, Sinclair G, Stockler-Ipsiroglu S, et al. The genotypic and phenotypic spectrum of PIGA deficiency. *Orphanet J Rare Dis [Internet]* 2015 [cited 2015 Mar 25];10(1). Available from: <http://www.orphandis.com/content/10/1/23>
40. Kevelam SH, Taube JR, van Spaendonk RML, et al. Altered PLP1 splicing causes hypomyelination of early myelinating structures. *Ann Clin Transl Neurol* 2015;2(6):648–61.
41. Zaharieva IT, Thor MG, Oates EC, et al. Loss-of-function mutations in SCN4A cause severe foetal hypokinesia or “classical” congenital myopathy. *Brain J Neurol* 2015;
42. Ogunbayo OA, Zhu Y, Rossi D, et al. Cyclic adenosine diphosphate ribose activates ryanodine receptors, whereas NAADP activates two-pore domain channels. *J Biol Chem* 2011;286(11):9136–40.
43. Rossi D, Simeoni I, Micheli M, et al. RyR1 and RyR3 isoforms provide distinct intracellular Ca²⁺ signals in HEK 293 cells. *J Cell Sci* 2002;115(Pt 12):2497–504.
44. van der Ham M, Prinsen BHCMT, Huijman JGM, et al. Quantification of free and total sialic acid excretion by LC-MS/MS. *J Chromatogr B Analyt Technol Biomed Life Sci* 2007;848(2):251–7.

45. Janer A, van Karnebeek CD, Sasarman F, et al. RMND1 deficiency associated with neonatal lactic acidosis, infantile onset renal failure, deafness, and multiorgan involvement. *Eur J Hum Genet* 2015;
46. Zhang X, Ling J, Barcia G, et al. Mutations in QARS, encoding glutaminyl-tRNA synthetase, cause progressive microcephaly, cerebral-cerebellar atrophy, and intractable seizures. *Am J Hum Genet* 2014;94(4):547–58.
47. Furukawa F, Tseng Y-C, Liu S-T, et al. Induction of Phosphoenolpyruvate Carboxykinase (PEPCK) during Acute Acidosis and Its Role in Acid Secretion by V-ATPase-Expressing Ionocytes. *Int J Biol Sci* 2015;11(6):712–25.
48. Adams DR, Yuan H, Holyoak T, et al. Three rare diseases in one Sib pair: RAI1, PCK1, GRIN2B mutations associated with Smith-Magenis Syndrome, cytosolic PEPCK deficiency and NMDA receptor glutamate insensitivity. *Mol Genet Metab* 2014;113(3):161–70.
49. SØvik O, Vidnes J, Falkmer S. Persistent neonatal hypoglycaemia. A clinical and histopathological study of three cases treated with diazoxide and subtotal pancreatectomy. *Acta Pathol Microbiol Scand [A]* 1975;83(1):155–66.
50. Richards S, Aziz N, Bale S, et al. Standards and guidelines for the interpretation of sequence variants: a joint consensus recommendation of the American College of Medical Genetics and Genomics and the Association for Molecular Pathology. *Genet Med Off J Am Coll Med Genet* 2015;17(5):405–23.
51. Pfützer R, Myers E, Applebaum-Shapiro S, et al. Novel cationic trypsinogen (PRSS1) N29T and R122C mutations cause autosomal dominant hereditary pancreatitis. *Gut* 2002;50(2):271–2.
52. Pérez B, Mechinaud F, Galambrun C, et al. Germline mutations of the CBL gene define a new genetic syndrome with predisposition to juvenile myelomonocytic leukaemia. *J Med Genet* 2010;47(10):686–91.
53. Bean LJH, Tinker SW, da Silva C, Hegde MR. Free the data: one laboratory's approach to knowledge-based genomic variant classification and preparation for EMR integration of genomic data. *Hum Mutat* 2013;34(9):1183–8.
54. Snoeckx RL, Huygen PLM, Feldmann D, et al. GJB2 mutations and degree of hearing loss: a multicenter study. *Am J Hum Genet* 2005;77(6):945–57.
55. Huculak C, Bruyere H, Nelson TN, Kozak FK, Langlois S. V37I connexin 26 allele in patients with sensorineural hearing loss: evidence of its pathogenicity. *Am J Med Genet A* 2006;140(22):2394–400.
56. Gentile M, Di Carlo A, Susca F, et al. COACH syndrome: report of two brothers with congenital hepatic fibrosis, cerebellar vermis hypoplasia, oligophrenia, ataxia, and mental retardation. *Am J Med Genet* 1996;64(3):514–20.
57. Brancati F, Iannicelli M, Travaglini L, et al. MKS3/TMEM67 mutations are a major cause of COACH Syndrome, a Joubert Syndrome related disorder with liver involvement. *Hum Mutat* 2009;30(2):E432–42.

58. Schuurs-Hoeijmakers JHM, Oh EC, Vissers LELM, et al. Recurrent de novo mutations in PACS1 cause defective cranial-neural-crest migration and define a recognizable intellectual-disability syndrome. *Am J Hum Genet* 2012;91(6):1122–7.
59. Niemela JE, Lu L, Fleisher TA, et al. Somatic KRAS mutations associated with a human nonmalignant syndrome of autoimmunity and abnormal leukocyte homeostasis. *Blood* 2011;117(10):2883–6.
60. Pao W, Wang TY, Riely GJ, et al. KRAS mutations and primary resistance of lung adenocarcinomas to gefitinib or erlotinib. *PLoS Med* 2005;2(1):e17.